

5-2023

Hydrological Modeling for the Impact of Predicted Climate Change and Urbanization: A Case Study of the Lower Mississippi River Basin

Amelie E. Lagarde
aelagard@uno.edu

Follow this and additional works at: <https://scholarworks.uno.edu/td>



Part of the [Hydraulic Engineering Commons](#)

Recommended Citation

Lagarde, Amelie E., "Hydrological Modeling for the Impact of Predicted Climate Change and Urbanization: A Case Study of the Lower Mississippi River Basin" (2023). *University of New Orleans Theses and Dissertations*. 3070.

<https://scholarworks.uno.edu/td/3070>

This Thesis is protected by copyright and/or related rights. It has been brought to you by ScholarWorks@UNO with permission from the rights-holder(s). You are free to use this Thesis in any way that is permitted by the copyright and related rights legislation that applies to your use. For other uses you need to obtain permission from the rights-holder(s) directly, unless additional rights are indicated by a Creative Commons license in the record and/or on the work itself.

This Thesis has been accepted for inclusion in University of New Orleans Theses and Dissertations by an authorized administrator of ScholarWorks@UNO. For more information, please contact scholarworks@uno.edu.

Hydrological Modeling for the Impact of Predicted Climate Change and Urbanization: A Case
Study of the Lower Mississippi River Basin

A Thesis

Submitted to the Graduate Faculty of the
University of New Orleans
in the partial fulfillment of the
requirements for the degree of

Master of Science in Engineering
in
Civil Engineering

by

Amelie Lagarde
B.S. University of Alabama, 2020

May 2023

Acknowledgement

This study received support from a project funded by the Board of Regents (Contract no: LEQSF (2022-25)-RD-A-28) titled “Quantifying potential Tradeoff and Synergies Between Food, Water, and Carbon Footprint Under Range of Water Management and Climate Change Scenarios, in the Lower Mississippi River Basin.”

Table of Contents

Acknowledgement	ii
Table of Contents	iii
List of Figures	v
List of Tables	ix
Abstract	x
Chapter 1: Introduction	1
Chapter 2: Literature Review	3
Chapter 3 Goals and Objectives.....	8
Methodology Chapter 4	9
4.1 Introduction	9
4.2 Site Area.....	9
4.3 SWAT model.....	14
4.4 Subbasin Creation: QGIS and QSWAT	16
4.5 SWAT Editor 2012.....	22
4.5.1 Weather Stations.....	23
4.5.1.1 Rainfall Data	24
4.5.1.2 Temperature Data	25
4.5.2 Writing Input Tables.....	26
4.5.3 SWAT Simulation	27
4.5.4 Calibration	29
4.5.5 Calibration Data.....	30
4.5.5.1 Observed Precipitation.....	30
4.5.5.2 Observed Out Flow.	31
4.6 SWAT Cup.....	32
4.6.1 Sensitivity Analysis	32
4.6.2 SWAT Cup Setup	33
4.6.3 Evaluation of Model performance using NSE metric	34
4.6.4 Validation	36
4.7 Climate Change and Hydrological Response.....	37
4.7.1 Future Climate Data.....	37
4.7.2 Future projection using calibrated SWAT Model	38
4.7.3 USACE’s Climate Hydrology Assessment	39

4.8 Land use and Hydrological Response	40
4.8.1 Land Use Data	40
4.8.2 Hydrological simulation of SWAT Model	41
Chapter 5: Results and Discussion.....	42
5.1 Climate Change and Hydrological Response.....	42
5.1.1 Model Response to RCP 2.6 vs 8.5	43
5.1.1.1 Model Simulation for 2040 Period	44
5.1.1.1.1 Streamflow	44
5.1.1.1.2 Evapotranspiration	44
5.1.1.1.3 Groundwater	45
5.1.1.2 Model Simulation for 2080 Period	46
5.1.1.2.1 Streamflow	46
5.1.1.2.2 Evapotranspiration	47
5.1.1.2.3 Groundwater	48
5.2 Hydrological Simulation: Future periods (2040s and 2080s)	49
5.1.2.1 Comparisons for RCP 2.6	49
5.1.2.1.1 Streamflow at the basin outlet.....	49
5.1.2.1.2 Evapotranspiration	50
5.1.2.1.3 Groundwater	51
5.1.2.2 Hydrological response simulated with RCP 8.5	52
5.1.2.2.1 Streamflow	52
5.1.2.2.2 Evapotranspiration	53
5.1.2.2.3 Groundwater flow	54
5.2 Hydrological Simulation: Land Use Change	55
5.2.1 Simulated Streamflow	56
5.2.2 Evapotranspiration.....	58
5.2.3 Groundwater flow.....	60
Chapter 6: Summary and Conclusion	62
Chapter 7: Recommendations for Future Research	65
References.....	67
Vita.....	72

List of Figures

Figure 4.1: USGS site 0736500	10
Figure 4.2: Forest Legacy Areas	11
Figure 4.3: 2040-2060 change in temperature with an RCP of 2.6	12
Figure 4.4: 2040-2060 change in temperature with an RCP of 8.5	12
Figure 4.5: 2080-2100 change in temperature with an RCP of 2.6	12
Figure 4.6: 2080-2100 change in temperature with an RCP of 8.5	12
Figure 4.7: Annual- mean 1 day temperature	13
Figure 4.8: Annual-maximum 1 day precipitation	14
Figure 4.9: QSWAT Dialog box pro delineating watershed, creating HRUs, editing and running SWT model and visualizing results	17
Figure 4.10: Figure 4.9: Dialog box for configuring the model domain based on the Selected DEM	18
Figure 4.11: Configuration of sub watershed	19
Figure 4.12: QSWAT dialogbox for creating Hydrologic response unit (HRU)	20
Figure 4.13: Land use map for the selected River basin (USGS ID 07363500)	21
Figure 4.14: The soil map for this study region	22
Figure 4.15: Land use look up table csv file example	22
Figure 4.16: SWAT editor menu	23
Figure 4.17 SWAT editor dialog box for defining the weather data	24
Figure 4.18: pcp.txt example	25

Figure 4.19: pcp data.txt example	25
Figure 4.20: tmp.txt example	26
Figure 4.21: T data.txt example	26
Figure 4.22: Figure 4.21: Dialog box for Write SWAT Database Tables	27
Figure 4.23: Swat editor dialog box for Setingup and Running SWAT Model Simulator	28
Figure 4.24: SWAT output menu	29
Figure 4.25: Precipitation in mm for daily data from January 1, 1996 to December 31, 2003 for USC site number 00033862.	31
Figure 4.26 Average daily flow rate in cubic meters per second (cms) from January 1, 1997 to December 31, 2002,at USGS site number 07363500.	32
Figure 4.27 Simulated average monthly flow rate in cubic meters per second (cms) from January 1, 1997 to December 31, 2002 at the outlet of the river basin 007363500	35
Figure 4.28 Observed and the simulated average monthly flow rate in cubic meters per second (cms) from January 1, 1997 to December 31, 2002 at river basin outlet (USGS ID 07363500)	35
Figure 4.29 Line chart showing the simulated and observed flow during the validation period	36
Figure 4.30: Simulated Annual-streamflow volume	40
Figure 5.1 Monthly average flow in cubic meters per second for river basin 07363500 from years 2045 – 2059 for both RCP 2.6 and RCP 8.5 scenario.	44

Figure 5.2 Monthly average evapotranspiration in millimeters per day for river basin 07363500 from years 2045 – 2059 for both RCP of 2.6 and 8.5	45
Figure 5.3 Monthly average groundwater flow in millimeters per day for subbasin 07362000 from years 2045 – 2059 for both RCP2.6 and RCP 8.	46
Figure 5.4 Monthly average flow in cubic meters per second for subbasin 07363500 from years 2085 – 2099 for both RCP 2.6 and RCP 8.5.	47
Figure 5.5 Monthly average evapotranspiration in millimeters per day for subbasin 07363500 from years 2085 – 2099 for both RCP 2.6 and RCP 8.5	48
Figure 5.6 Monthly average groundwater flow in millimeters per day for subbasin 07362000 from years 2085 – 2099 for both RCP 2.6 and RCP 8.5.	49
Figure 5.7 Monthly average flow in cubic meters per second for subbasin 07363500 with RCP 2.6 from year 1 (2045 for 2040 data and 2085 for 2080 data) through year 15 (2059 for 2040 data and 2099 for 2080 data)	50
Figure 5.8 Monthly average evapotranspiration in millimeters per day for subbasin 07363500 with RCP 2.6 from year 1 (2045 for 2040 data and 2085 for 2080 data) through year 15 (2059 for 2040 data and 2099 for 2080 data).	51
Figure 5.9 Monthly average groundwater in millimeters per day for subbasin 07363500 with RCP 2.6 from year 1 (2045 for 2040 data and 2085 for 2080 data) through year 15 (2059 for 2040 data and 2099 for 2080 data).	52
Figure 5.10 Monthly average groundwater flow in cubic meters per second for subbasin 07363500 with RCP 8.5 from year 1 (2045 for 2040 data and 2085 for 2080 data) through year 15 (2059 for 2040 data and 2099 for 2080 data).	53
Figure 5.11 Monthly average evapotranspiration in millimeters per day for subbasin 07363500 with RCP 8.5 from year 1 (2045 for 2040 data and 2085 for 2080 data) through year 15 (2059 for 2040 data and 2099 for 2080 data).	54

Figure 5.12 Monthly average groundwater in millimeters per day for subbasin 07363500 with RCP 8.5 year 1 (2045 for 2040 data and 2085 for 2080 data) through year 15 (2059 for 2040 data and 2099 for 2080 data).	55
Figure 5.13 Monthly average flow in cubic meters per second for subbasin 07363500 for 100% Forest (FRST) land use and 100% URBN (Urban) land use.	57
Figure 5.14 Monthly average flow in cubic meters per second in the year 2045 for subbasin 07363500 for varying land uses.	58
Figure 5.15 Monthly average evapotranspiration in millimeters per day for subbasin 07363500 for 100% Forest (FRST) land use and 100% Urban (URBN) land use.	59
Figure 5.16 Monthly average evapotranspiration in millimeters per day second in the year 2045 for subbasin (USGS ID 07363500) for two land use scenarios (completely Forest (FRST) and Completely urban (URBN)).	60
Figure 5.17 Monthly average groundwater flow in millimeters per day for subbasin 07363500 for 100% Forest (FRST) land use and 100% (URBN) Urban land use.	61
Figure 5.18 Monthly average groundwater flow in millimeters per day second in the year 2045 for subbasin 07363500 for varying land uses.	61

List of Tables

Table 4.1: Table showing the soil ID and % of watershed occupied.	22
Table 4.2: Parameter change method maximum and minimum values for calibration	33
Table 4.3: Table 4.3: HRU calibrated parameter values	33
Table 4.4: List of calibrated parameter value changes	36
Table 5.1: Model Simulation Summary of flow, evapotranspiration, and groundwater for 2040 and 2080 period	43
Table 5.2: Results for Objective 2	56

Abstract

The Mississippi River Basin is the United States' largest watershed and consists of many subbasins. Each subbasin has hydrological processes including flow rate, evapotranspiration, and groundwater flow. It is important to understand how these processes change through shifts in weather, time, and land use.

This study uses the Soil and Water Assessment Tool (SWAT) to predict how changes in temperature, rainfall, and land use can change hydrological processes responses. This study concludes that, for the studied subbasin, a high representative concentration pathway (RCP) will result in lower flow rates and ground water flow as well as higher evapotranspiration by the year 2080. Additionally, as this area becomes urbanized, the average flow rate can be expected to increase by 3.07cms with 106.12cms higher peak flow, the evapotranspiration can be expected to have a peak flow of 1.01mm/day higher, and the average ground water can be expected to drop by 0.85mm/day.

Key Words: Climate Change, Hydrological Response, SWAT Model, Land Use

Chapter 1: Introduction

Recent years have shown an increase in the studying of the hydrological response to the changing environment and climate. This is partly due to the 2001 Hypoxia Task Force Action Plan created to address the growing hypoxic zone in the Gulf of Mexico that is growing due to the outflow of the Mississippi River (Third Gulf of Mexico Hypoxia Task Force, NCCOS; Hypoxia Task Force Action Plans, EPA).

For the United States, understanding the Mississippi River Basin is crucial to understanding the hydrological systems in the country (MARB). This is due to the Mississippi River draining over 1,245,000 square miles of the United States and parts of Canada (MARB, EPA). It is the third largest river basin in the world covering 41% of the continental United States and 15% of North America (MARB, EPA). All the water that falls in this area gets transported through the regional streams and tributaries that are connected and empty into the Mississippi River (MARB, EPA).

Each of these tributaries creates its own subbasin. According to the US Army Corps of Engineers (USACE), a subbasin is defined as “an element that usually has no inflow and only one outflow” (Hydrologic Modeling System, USACE). The water flow in these areas is driven by the precipitation and flows into one outflow point which becomes an input to the Mississippi River. Each of these input points carries with it a unique sediment load, water quantity, and pollutants of varying toxicity and hazards (Moody and Battaglin, 1995). The makeup and concentration of these sediment inflows influences the entire downstream of the Mississippi River (Moody and Battaglin, 1995).

Due to the effect that subbasins have on all downstream areas, it is important to study the hydrological processes of these subbasins and determine how such processes are changed by

different factors. Such changes can come from physical factors, such as land use and soil make up, as well as weather changes such as rainfall and temperature (Phung et al., 2019; Neupane and Kumar 2015; Serpa et al., 2015, Parajuli, 2010).

The warming of climate can cause a hydrological responses such as creating algae blooms (Gobler, 2020). Such alterations could threaten food, water quality, local economy, and human health (Gobler, 2020). Additionally, climate change can influence sediment load which will impact the makeup of rivers and other bodies of water (Cousiono et al., 2005). Additionally, a difference in land use can also influence hydrological processes (Miller et al., 2002). These changes in hydrological processes can be predicted through hydraulic modeling.

Chapter 2: Literature Review

Conceptual rainfall-runoff (CRR) models are coupled with global climate models (GCM) to simulate the hydrological response. The CRR models use climate data simulated by GCM to drive the hydrological response (Kour and Patel, 2016).

CRR models take the complexity of water, energy, and vegetation processes and, through a series of equations, can project the future outputs of a watershed system (Kour and Patel, 2016). Hydrological conceptual models are a useful tool in studying hydrological systems. They have been widely used to study how a hydrological system changes in response to factors such as pollutants (Santhi et al., 2006; White et al., 2014), land use and land management (Betrie et al., 2011; Millet et al., 2002), and climate change (Muttiah and Wurbs, 2002; Cousiono et al., 2015).

There are many widely utilized conceptual models for simulating hydrological systems such as MIKE SHE, SWMM, and AnnAGNPS (Arhonditsis et al., 2019). However, the most widely utilized model for simulating a hydrological system is the Soil and Water Assessment Tool (SWAT) model (Arnold et al., 1998; Arnold and Fohrer, 2005, Ougahi et al., 2002).

The SWAT model is widely used to study environmental concerns (Gassman et al., 2007), especially in the United States where it is used with the USDA for conservation studies (Gassman et al., 2007). The SWAT model is user friendly with many forums to help with processing issues, has given global data sets (Global Data, <https://swat.tamu.edu/data/>), and a variety of calibration programs and other supporting software systems (Ougahi et al., 2002).

SWAT utilizes a continuous daily time step to determine the changes of a watershed system due to both physical and weather changes within the system (Gassman et al., 2007). There are 8 main components in the SWAT model. These components are climate, hydrology, nutrients and pesticides, erosion, land use and vegetation, management practices,

channel processes, and bodies of water (Gassman et al., 2007). The SWAT model relies heavily on creating a water balance assessment due to the influence it has on many different parameters within the model such as plant growth and sediment movement- which carries with it a variety of distinct nutrients, pesticides, and pathogens (Gassman et al., 2007).

The SWAT model utilizes HRUs, hydraulic response units, in its system to calculate outputs (Gassman et al., 2007). HRUs further breakdown the subbasin based on similar land use, soil, and elevation in the area. This allows more than one land use and soil type to be present in each subbasin and allows for reliable long-term modeling (Arnold et al., 2012b).

The SWAT model is highly regarded and widely used for a variety of different studies. Muttiah and Wurbs (2002) used the SWAT model to study a watershed in Texas in the San Jacinto River Basin. This study focused on a single time period from the years 2040-2059 and compared the output data to historical data for the subbasin (Muttiah and Wurbs, 2002). This study found that the long term mean stream flows were higher in the future projected data during times of floods and high flow. However, it found that the projected flow data was lower in periods of normal and low flow in comparison to the historical data (Muttiah and Wurbs, 2002).

Another study completed in 2002 looks at watersheds in Arizona and New York (Miller et al., 2002). This study uses the SWAT model to determine how the steam flow is affected by land use (Miller et al., 2002). While two watersheds are used, they are both studies in a unique way. The Arizona watershed looks at an increase in urban and agriculture land and saw an increase in stream flow (Miller et al., 2002). However, the New York watershed has a land use shift from agricultural to forested causing a decrease in stream flow (Miller et al., 2002).

Gassman et al., created a case study in 2007 studying various components of the SWAT model. In this study Gassman talks about the Nash-Sutcliffe model efficiency (NSE) and how it has been heavily relied upon for SWAT modeling (Gassman et al., 2007). This study points to the varying NSEs used throughout many studies (Gassman et al., 2007).

In 2012, Arnold et al created a case study looking at the calibration and validation of the SWAT model. This study talks about the importance of calibration and validation of a SWAT model as well as different ways the SWAT model can be calibrated (Arnold et al., 2012b). Additionally, this study walks through the usage of SWAT-CUP (calibration and uncertainty program), a calibration tool that utilizes a semiautomated approach (SURFI2) (Arnold et al., 2012b). Using SURFI2 with SWAT-CUP allows for a combination of manual and automatic calibration to take place (Arnold et al., 2012b). This allows the user to adjust parameters easily without manually calibrating the watershed (Arnold et al., 2012b).

A 2014 study observed hypoxic zone growing in the Gulf of Mexico (White et al., 2014). It has been understood that this hypoxic zone is a result of high levels of nutrients being inputted from the Mississippi River (White et al., 2014). Due to the nature of the industry, agricultural processes are high contributors to the high nutrient levels being added to the River (White et al., 2014).

This study utilized the SWAT model and was able to determine the nitrogen and phosphorus found in both local waters and the Gulf of Mexico were predominantly due to cropland (White et al., 2014). Additionally, it was determined a large amount of phosphorus levels could be traced back to point sources on the Tennessee and Arkansas/ Red River basins in addition to non-point urban sources. Results also concluded that Mississippi and Ohio were the largest contributors to nutrient deposits (White et al., 2014). The SWAT model was also able to

determine a high majority of nitrogen (87%) and phosphorus (90%) that was located near the mainstream of the Mississippi River were modeled to enter the Gulf of Mexico (White et al., 2014). Additionally, this study also looked at how agricultural conservation practices can be expected to change the nutrient load levels in the Gulf (White et al., 2014). It was modeled that certain conservation processes have the possibility to decrease such loads in the Gulf by 20% (White et al., 2014).

A study completed in 2015 uses the SWAT model to determine how climate change would affect the watershed yield in the Maumee River (Cousiono et al., 2015). This study looked at four Coupled Model Intercomparison Project Phase 5 models as the climate change data (Cousiono et al., 2015). The study found that in extreme climate change scenarios smaller flow reductions were found but with an increase of sediment load. The moderate scenarios had larger annual flow reductions as well as a reduction in sediment yields.

The SWAT model is widely used to model specific basins (Cousiono et al., 2015; Muttiah and Wurbs, 2002) and determine how hydrological processes are expected to change in that area. However, many of these studies focus only on the flow of the basin and ignore other hydrological processes such as evapotranspiration and ground water flow. Additionally, few studies look at how processes can change by looking at not only different climate change model extremes but also different periods of time.

This study will utilize similar methods study the study site (USGS ID 07363500). Two separate RCP scenarios of 2.6 and RCP 8.5 will be generated for periods 2040-2059 and 2080-2099. Additionally, the study will explore how hydrological processes will respond to urbanization. This study will focus on outflow, evapotranspiration, and ground water flow.

The studies mentioned in the above section show how the SWAT model has not only been successfully used, but is also the best model to use for this study due to its ease of use, available data, and calibration tools. Additionally, the above studies show how land use change and climate change can both be studied using the SWAT model.

Due to previous studies (Cousiono et al., 2015; Miller et al., 2002; Muttiah and Wurbs, 2002), it is predicted that the results of this study will show that climate change data will result in a decrease in peak flow and ground water flow with an increase in evapotranspiration for the more extreme scenario RCP 8.5 and for the later period starting in 2080. For a change in land use, an increase in stream flow and evapotranspiration and a decrease in groundwater is expected for more urbanized land uses.

Chapter 3 Goals and Objectives

Due to gaps in previous research (studies of hydrological processes besides flow rate, lack of studies that look at climate and land use change), the main objective of this research was to evaluate how the hydrological processes of flow rate, evapotranspiration, and ground water flow in this subbasin are affected by changes to both the weather patterns due to climate change and land use.

The above objective was met by accomplishing the following specific goals:

1. Determining how out flow, groundwater flow, and evapotranspiration changed based on different future climate change projections (RCP 2.6 and 8.5 for years 2040-2059 and 2080-2099).
2. Determining how out flow, groundwater flow, and evapotranspiration changed based on an urbanized change in land use.

Methodology Chapter 4

4.1 Introduction

There were two objectives to this research, both with the goal of determining how the hydrological processes of flow rate, groundwater flow, and evapotranspiration were affected by changes in the physical character of the subbasins. The first objective was to determine the effects of future climate change projections by utilizing projected temperature and precipitation data. The second objective was to determine how land use, specifically through the process of urbanization, could affect these processes. This was done by utilizing a series of modified land use maps.

To explore the effect of climatic changes on hydrological response, future projected temperature and precipitation scenarios were synthetically created and forced through the calibrated model. Different land use maps were also used to explore the sensitivity of land use changes on model response.

Several publicly available GIS-based tools, e.g., QGIS, QSWAT, SWAT Editor, and SWAT-CUP were used to preprocess model input, setup model simulation, and post-process model output. This chapter will describe the data and methods used to run the models performed.

4.2 Site Area

This study selected small size river basins unaffected by human activities from the Lower Mississippi river basin. The river basin selected from this study is the Saline River and the streamflow data corresponding to USGS site USGS site 07363500 is used. It is located in central-south Arkansas in close proximity to the Mississippi River. The location of the site's outflow point is near Rye, Arkansas, at a decimal latitude, and longitude of 33.70, -92.03 (Saline

River, USGS). The main river in the subbasin is the Saline River (Saline River, USGS). The process of the DEM to extract the river basin corresponding to the USGS outlet location produced a catchment area of the size of 1,336,283 acres. Figure 4.1 shows the location of the selected river basin (Saline River, USGS).



Figure 4.1: USGS site 0736500 This is a map of the studied site in central-south Arkansas taken from the USGS website <https://waterdata.usgs.gov/monitoring-location/07363500/#parameterCode=00065&period=P7D>.

The river basin is a tributary of the Mississippi River. Additionally, choosing the subbasin, which is in Arkansas, allowed the study of an area that is in the southern Mississippi River Valley but also contains little to no wetlands, which adds many unknown and quickly changing variables to the model.

A 1987 study of the lower Ouachita Basin includes this area as well as some additional areas southeast of the studied subbasin (Arkansas State Water Plan, 1987). The study found the following: 84% of the land was forest land and 5.9% was dedicated to cropland (Arkansas State

Water Plan, 1987). The area has land that is gently rolling (Arkansas State Water Plan, 1987). A concern for this area is seasonal low flow events in the summer which has caused issues with the agricultural farming in the area (Arkansas State Water Plan, 1987). Additionally, there are some water quality concerns from non-point solutions such as agriculture, strip mining, soil, and silviculture in the area (Arkansas State Water Plan, 1987). Finally, large amounts of ground water have been extracted from aquifers for irrigation, public supplies, and industry usage (Arkansas State Water Plan, 1987).

This study area is within the Lower Mississippi River Basin region and is experiencing changing climate and land use patterns. The Arkansas Department of Agriculture's 2020-2029 Forest Action Plan eight forest legacy areas as areas most at risk of urbanization. This includes areas within the studied subbasin as seen in figure 4.2 (Arkansas 2020-2029 Forest Action Plan, Arkansas Department of Agriculture).

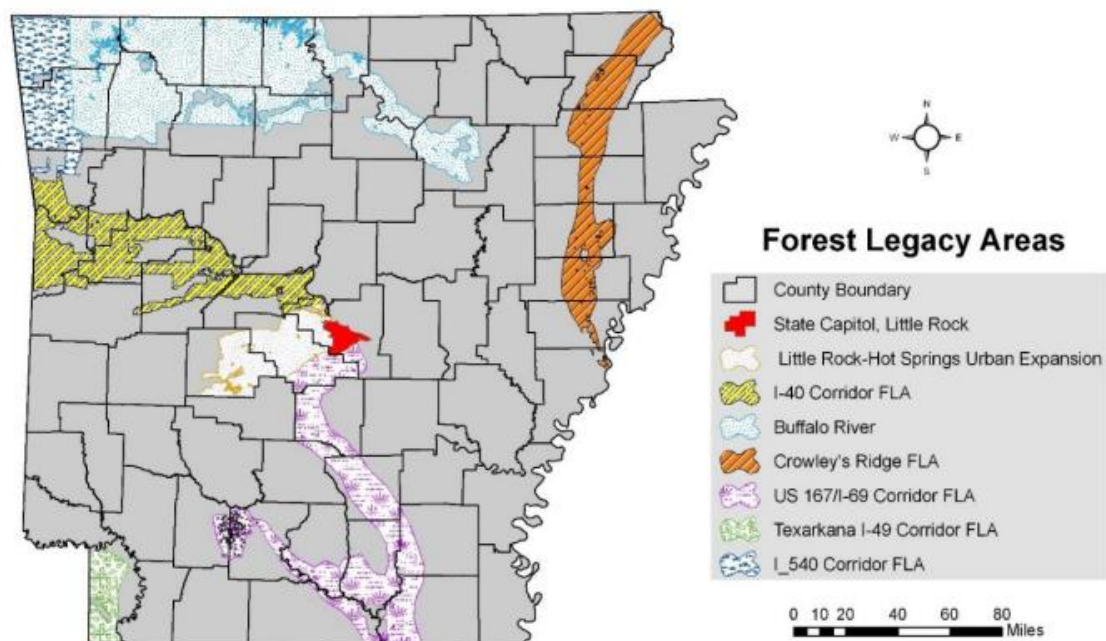


Figure 4.2: Forest Legacy Areas map from the Arkansas Department of Agriculture's 2020-2029 Forest Action Plan showing the forest legacy areas which were determined to be the areas most

at risk of urbanization. <https://www.agriculture.arkansas.gov/wp-content/uploads/2021/01/Arkansas-Forest-Action-Plan.pdf>

In addition to land use changes, many climate change models indicate that this area- will experience warming periods in the future. Figure 4.3 shows the mean temperature change from the years 2040-2060 (projected with an RCP 2.6) minus the observed 1986-2005 data. Figure 4.4 shows the same with an RCP of 8.5. Figure 4.5 shows an RCP 2.6 for the years 2080-2100 and Figure 4.6 is it's counterpart for RCP 8.5. Maps created used GCM: CMIP5 and were created by KNMI Climate Change Atlas ([KNMI Climate Change Atlas, Climate Explorer](#)).

mean rcp26 temperature 2040-2060 minus 1986-2005 Jan-Dec AR5 CMIP5 subset

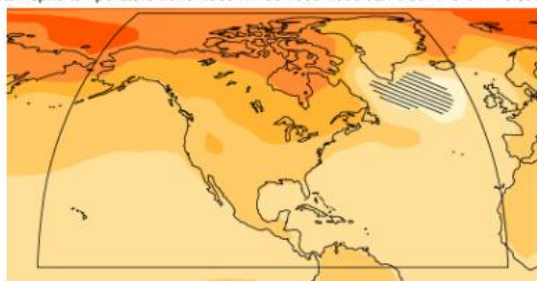


Figure 4.3: 2040-2060 change in temperature with an RCP of 2.6 Map calculated from http://climexp.knmi.nl/plot_atlas_form.py.

mean rcp85 temperature 2040-2060 minus 1986-2005 Jan-Dec AR5 CMIP5 subset

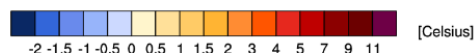
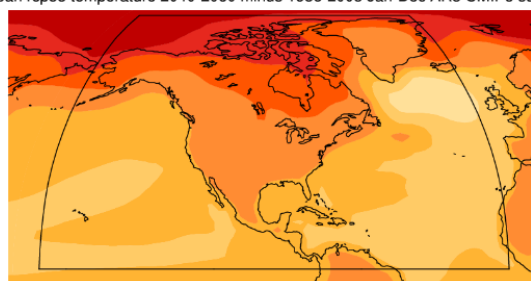


Figure 4.4: 2040-2060 change in temperature with an RCP of 8.5 Map calculated from http://climexp.knmi.nl/plot_atlas_form.py.

mean rcp26 temperature 2080-2100 minus 1986-2005 Jan-Dec AR5 CMIP5 subset

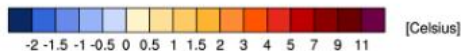
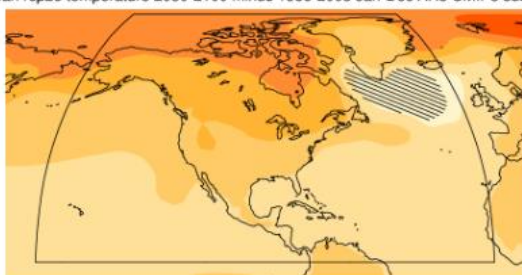


Figure 4.5: 2080-2100 change in temperature with an RCP of 2.6 Map calculated from http://climexp.knmi.nl/plot_atlas_form.py.

mean rcp85 temperature 2080-2100 minus 1986-2005 Jan-Dec AR5 CMIP5 subset

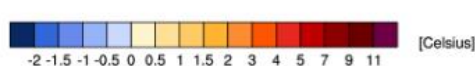
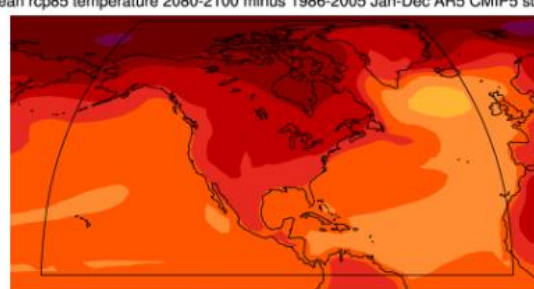


Figure 4.6: 2080-2100 change in temperature with an RCP of 8.5 Map calculated from http://climexp.knmi.nl/plot_atlas_form.py.

Figure 4.7 uses the USACE's Climate Hydrology Assessment Tool was used to obtain a visual of projected temperature change. The HUC 08040204 was used to get the data at the outflow of the studied subbasin (Climate Hydrology Assessment Tool, USACE).

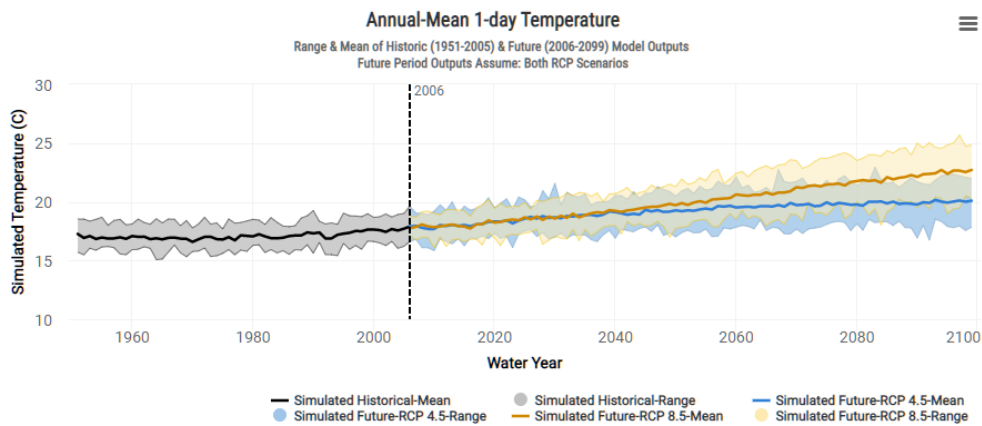


Figure 4.7: Annual- mean 1 day temperature This graph shows how the temperature has been observed and is expected to change through the year 2100 for RCP 4.5 and 8.5. This image is from USACE's Climate Hydrology Assessment Tool founded on the website: <https://climate.sec.usace.army.mil/chat/>.

Finally, along with temperature change, precipitation change is also expected to occur. The USACE's Climate Hydrology Assessment Tool was used to obtain visuals for precipitation change. The HUC 08040204 was used to get the data at the outflow of the studied subbasin. Figure 4.8 shows the simulated monthly mean and range for RCP 4.5 and 8.5.

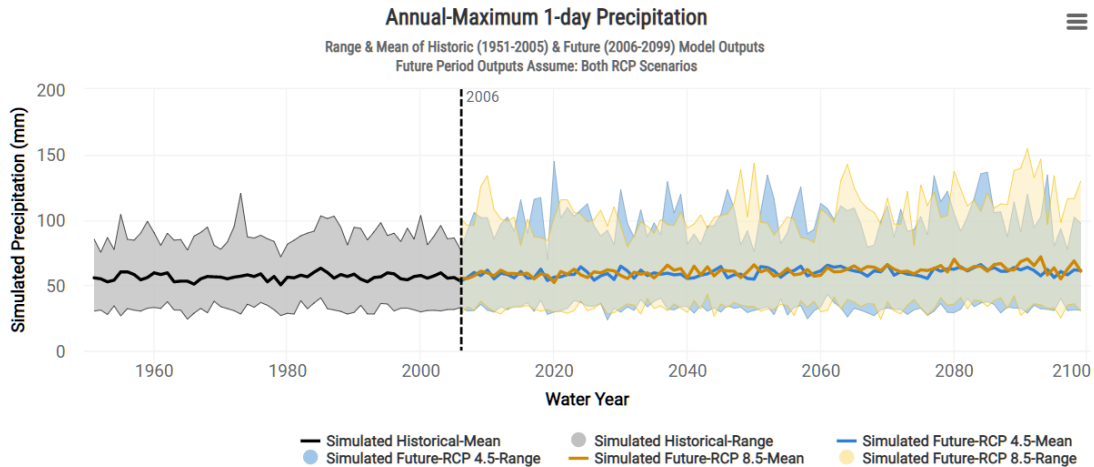


Figure 4.8: Annual-maximum 1 day precipitation This graph shows how the precipitation has been observed and is expected to change through the year 2100 for RCP 4.5 and 8.5. This image is from USACE's Climate Hydrology Assessment Tool founded on the website: <https://climate.sec.usace.army.mil/chat/>.

4.3 SWAT model

There are many models that can be utilized to estimate and project what the outflow of a specific sub basin will be composed of. For this project, the SWAT model was used.

As discussed in chapter 2, there are many positives to using the SWAT model including the ease of use and support, accessibility to global data on the SWAT website, and many calibration tools to choose from. Additionally, the SWAT model gives consistent long-term estimates and streamflow estimates for many different climate conditions (Gassman, 2012).

SWAT was created to predict and study how land management would impact water, sediment, and chemical yields on a large scale (complex and large watersheds over long periods of time) (Hydrological Modeling with SWAT, BTU). SWAT divides a watershed into smaller subbasins (Gassman , 2012). Within the subbasins are even smaller hydrological response units (HRUs) which are created based on land use, management, and soil data (Gassman, 2012; Arnold et al., 2012a). While the subbasins are spatially represented within the watershed the HRUS are not but instead represent a percentage of a subbasin within the watershed (Arnold et

al., 2012a). This makes the SWAT model a semi-distributed physically based model and adds accuracy to load predictions (Hydrological Modeling with SWAT, BTU).

Along with HRUs, within each of the watershed's subbasin, SWAT recognizes a single reach: the main channel segments (Arnold et al., 2012a). Additionally, a single pond, a single wetland, impoundments that are connected to the main channel network, and point sources can be identified for each subbasin though these are not used in this study (Arnold et al., 2012a).

SWAT uses a combination of user-inputted data and simulated data to run. There are two hydrological components that SWAT considers. These are soil and land use hydrology and channel hydrology (Rashid, 2014). The soil hydrology is calculated for each HRU using the following equation (Arnold et al., 1998, Hydrological Modeling with SWAT, BTU; Rashid, 2012):

$$SW_t = SW_0 + \sum_{i=1}^t R_{day} - Q_{surf} - E_a - w_{seep} - Q_{gw}$$

Where SW_t is the final soil water content, SW_0 is the initial soil water content, R_{day} is the precipitation, Q_{surf} is the surface runoff, E_a is the evapotranspiration, w_{seep} is the percolation flow exiting the soil bottom, and Q_{gw} is the ground water flow (Hydrological Modeling with SWAT, BTU).

The surface runoff is calculated using the U.S. Soil Conservation Society (SCS) curve number method. A curve number is determined by both the hydraulic soil group and the land use (Hydrological Modeling with SWAT, BTU; Rashid, 2014). A higher curve number creates a higher potential of runoff (Hydrological Modeling with SWAT, BTU). In SWAT, the curve number is combined with the rainfall data (either simulated or observed) to receive a runoff in mm (Hydrological Modeling with SWAT, BTU).

SWAT calculates the potential evapotranspiration using the Penmen-Montheith method. This method uses the solar radiation, soil heat flux density, psychrometric constant, wind speed, relative humidity, and air temperature to determine the potential evapotranspiration (Hydrological Modeling with SWAT, BTU).

SWAT requires eight inputs to run. These climate inputs are: precipitation, temperature, windspeed, soar radiation, relative humidity. These inputs can either be simulated by SWAT or inputted by the user. In this study observed precipitation and temperature were used. The last three required inputs are: land use, soil, and elevation. These three inputs must be used to create a watershed through QGIS (used in this study) or a like program (Hydrological Modeling with SWAT, BTU).

In order to run the SWAT model, first a subbasin needs to be created. Secondly, the model must be set up in a SWAT data base. Next, a calibration process must take place. Finally, the SWAT model is ready to be run.

4.4 Subbasin Creation: QGIS and QSWAT

The first step in running a SWAT Model is creating the subbasin representing the physical system. In this study, QGIS was used to create subbasins. Alternatively, this can also be performed in other GIS systems such as ArcGIS.

Creating a subbasin or the model domain for setting up SWAT model requires a digital elevation model (DEM), land use map, and soil map. These files are put into the SWAT plug-in (QSWAT) to create a file that the SWAT model can then read. Three main steps are followed by an optional visualization step to set up a model using QSWAT. The first step is to delineate the watershed, create HRUs, and edit inputs and run SWAT. The interface of QSWAT's menu can be seen in figure 4.9.

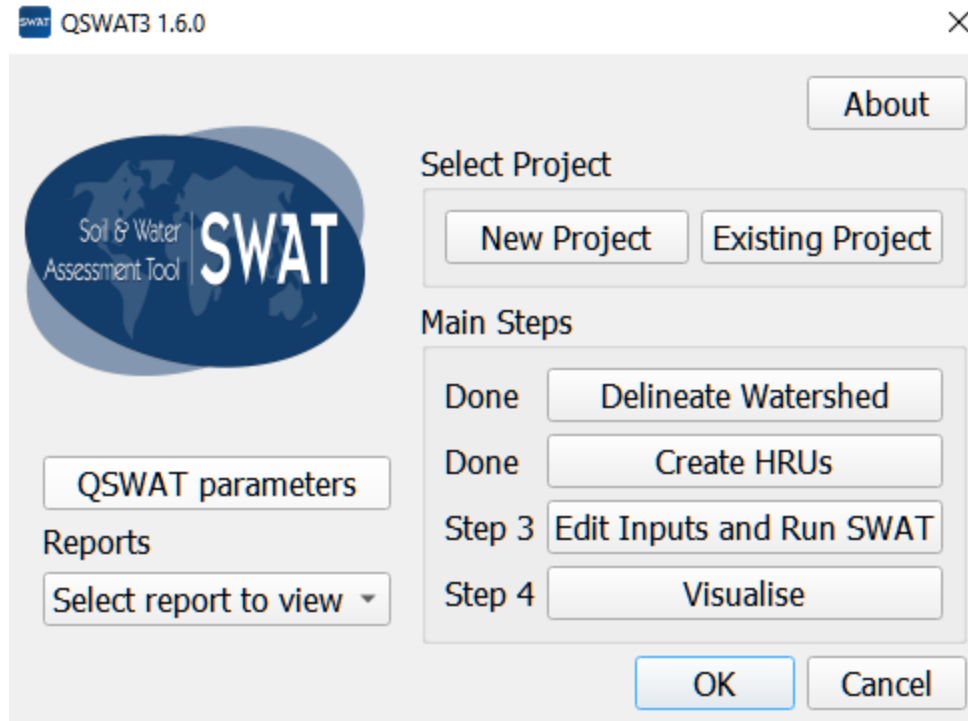


Figure 4.9: QSWAT Dialog box pro delineating watershed, creating HRUs, editing and running SWT model and visualizing results

Delineating the watershed creates the elevation map of the area of study. The DEM file in tiff format is put into QSWAT. The DEM data used in this study was from the United States Department of Agriculture’s geospatial data gateway site (Geospatial Data Gateway, USDA, https://datagateway.nrcs.usda.gov/GDGHome_CheckOrder.aspx). Once the DEM is loaded, there is an availability to change the sensitivity of the streams created. The lower the number of cells or area in the defined threshold, the more streams will be created as SWAT is processing the smaller steams. However, when loading your DEM, QSWAT will automatically estimate a threshold. The automated threshold was used in this study for both subbasins. Clicking the “Create streams” button (as seen in figure 4.10) creates the streams for the watershed. Next, the “Draw inlets/outlets” button (as seen in figure 4.10) is pressed, and an outlet is selected at the

desired point on a stream. Finally, pressing the “OK” button finished this first step. Figure 4.11 shows the created watershed. It consists of 11 subbasins with the outlet point in subbasin 1.

The image shows a software dialog box titled "Delineate Watershed". It has a "Select DEM" section at the top with a text field containing the file path "C:\Users\ameli\OneDrive\Desktop\0.66URBN\herewego\Source\dem.tif" and a browse button "...". Below this are four tabs: "Delineate watershed", "Use existing watershed", "DEM properties", and "TauDEM output". The "Delineate watershed" tab is selected and contains several options: a checkbox for "Burn in existing stream network" (unchecked), a "Define threshold" section with a text field "44768", a label "Number of cells", a text field "362.6", and a dropdown menu "Area [sq. km]", and a checkbox "Use an inlets/outlets shapefile" (checked) with a text field "C:\Users\ameli\OneDrive\Desktop\0.66URBN\herewego\Watershed\Shapes\drawoutlets.shp" and a browse button "...". There are also buttons for "Draw inlets/outlets", "Select inlets/outlets", "Review snapped", and "Create streams". At the bottom of the dialog are buttons for "Merge subbasins", "Merge", "Add reservoirs and point sources", "Add", "Number of processes" (set to 0), "Show Taudem output" (unchecked), "OK", and "Cancel".

Figure 4.10: Dialog box for configuring the model domain based on the Selected DEM

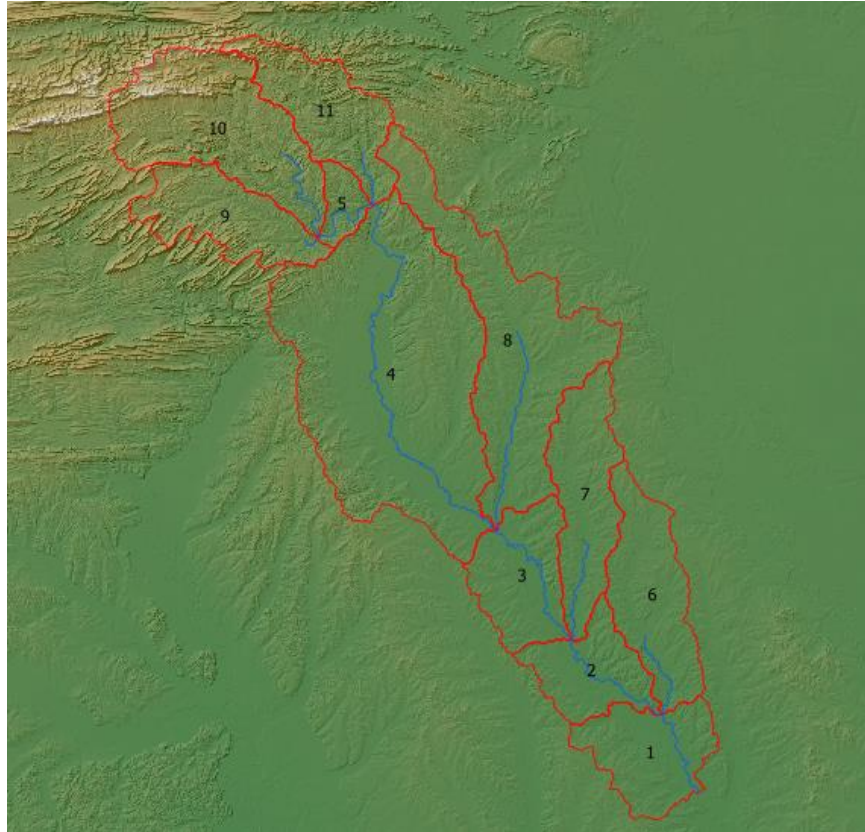


Figure 4.11: Configuration of sub watershed of the selected river basin (07363500). Also shown are the label for each subbasin.

Once the watershed is created the HRUs can be created by pressing the “Create HRUs” button (figure 4.9) on the QSWAT menu. Here, the land use map and soil map are selected (figure 4.12).

The land use and soil maps were taken from the soil data published on the SWAT website (Global Data, <https://swat.tamu.edu/data/>). The soil map was reprojected and scaled and does not accurately represent the site but instead very represents the five soils as seen below. However, the land use map was reclassified to create a simple land use map to simplify data processing. The land use map used consisted of 30.98% evergreen forest (FRSE) and 69.02% general forest land use (FRST). The land use map used can be seen in figure 4.13. The soil map can be seen in figure 4.14 and the soil watershed makeup percentages can be seen in Table 4.1.

Create HRUs

Select landuse map
 s:\ameli\OneDrive\Desktop\0.66URBN\herewego\Source\crop\landuse2.tif ...
 Landuse table Use csv file

Select soil map
 \Users\ameli\OneDrive\Desktop\0.66URBN\herewego\Source\soil\soIL.tif ...

Soil data
☒ usersoil ☐ STATSGO ☐ SSURGO/STATSGO2 Soil table global_soils

☐ Generate FullHRUs Read choice
 shapefile ☒ Read from maps ☐ Read from previous run

Read

Set bands for
 Insert

 Slope

Optional

Single/Multiple HRUs
☐ Dominant landuse, soil, slope
☒ Dominant HRU
☐ Filter by landuse, soil, slope
☐ Filter by area
☐ Target number of HRUs

Threshold method
☒ Percent of subbasin
☐ Area (Ha)

Set landuse, soil, slope thresholds
 0 Landuse (%) 100

 0 Soil (%) 100

 0 Slope (%) 100

Create HRUs Cancel

Figure 4.12: QSWAT dialogbox for creating Hydrologic response unit (HRU)

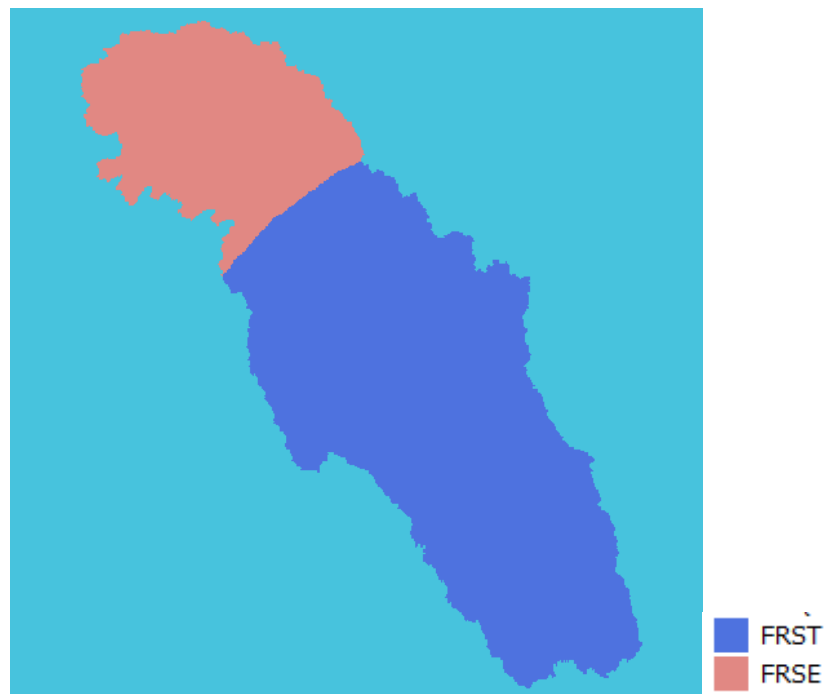


Figure 4.13: Land use map for the selected River basin (USGS ID 07363500)

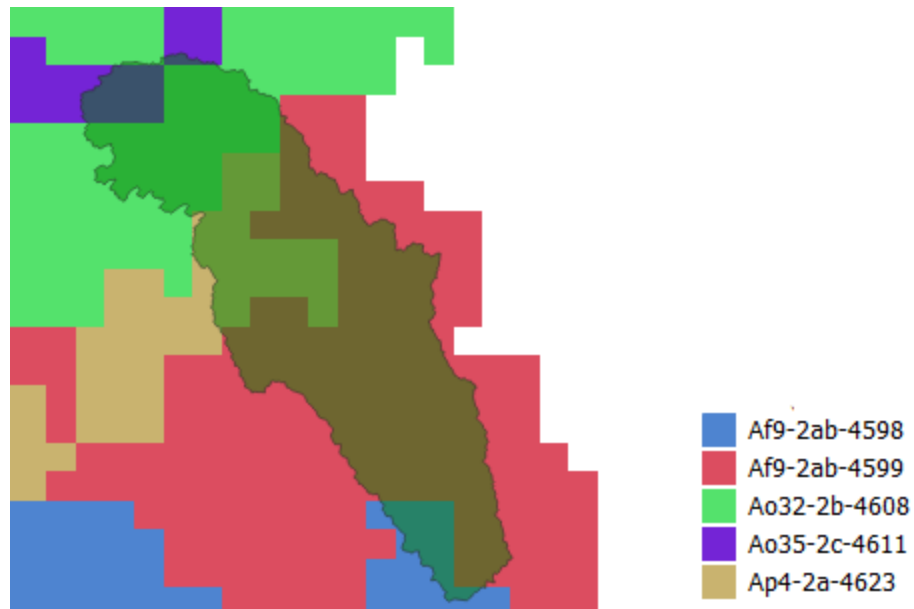


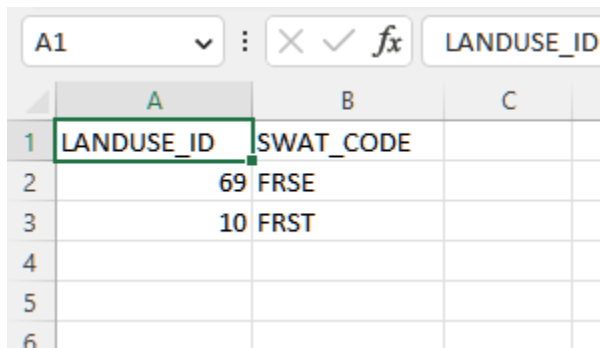
Figure 4.14: The soil map for this study river basin (USGS ID 07363500)

Soil ID	% of Watershed
Ao35-2c-4611	5.05%
Ao32-2b-4608	18.55%
Af9-2ab-4599	56.10%
Ap4-2a-4623	15.73%
Af9-2ab-4598	4.57%

Table 4.1: Table showing the soil ID and % of watershed occupied.

When inputting land use and soil tables, look up tables for both data sets must be chosen (figure 4.12). In this study, global soils were used. These tables were downloaded along with the SWAT programs (Global Data, <https://swat.tamu.edu/data/>).

However, since the land use map was reclassified an excel comma-separated value (csv) file was created and used. It contained two columns. The first contained the land use id as labeled in the imported land use map, and the second contained the SWAT code for the desired land use. An example of a land use lookup table can be found in figure 4.15. Once all maps and tables are selected the “Read” button (figure 4.12) is clicked followed by “Create HRUs”. This will complete the second step of SWAT setup.



	A	B	C
1	LANDUSE_ID	SWAT_CODE	
2	69	FRSE	
3	10	FRST	
4			
5			
6			

Figure 4.15: Land use look up table csv file example

Finally, “Edit Inputs and Run SWAT” (figure 4.9) is clicked, and the third step begins. Clicking this will open the QSWAT project in SWAT Editor 2012.

4.5 SWAT Editor 2012

The SWAT Editor program sets up the SWAT model. The first step is to connect to the databases needed. The first database is the SWAT Project GeoBase. This is the QSWAT file that was created in section 4.2 (it will automatically load when opened directly from QGIS). The second two databases are the SWAT parameter geodatabase and the SWAT soils database. Both databases are downloaded when downloading SWAT Editor and are found in the SWAT Editor folder under the name “SWAT 2012” (figure 4.16).

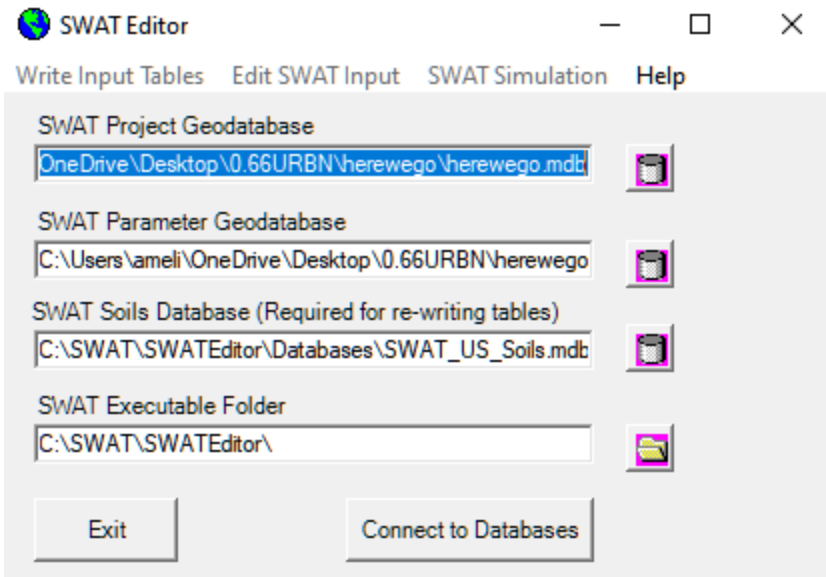


Figure 4.16: SWAT editor menu

Once connected to the database, the input tables are written. As mentioned above, SWAT allows for many parameters to be adjusted by adding observed data or to be simulated by the SWAT program.

4.5.1 Weather Stations

Under the write Input Tables tab is a weather data definition tab that allows for all weather data to be changed including: the relative humidity, solar radiation, wind speed, weather generators, rainfall, and temperature data (figure 4.17). For this research, the weather generator data that was chosen for all runs was “WGEN_US_COOP_1960_2010.” The cooperative observer program (COOP) is the national weather services’ data network that includes observed data from all types of areas (urban, farms, national parks, ect). (COOP, National Weather Service).

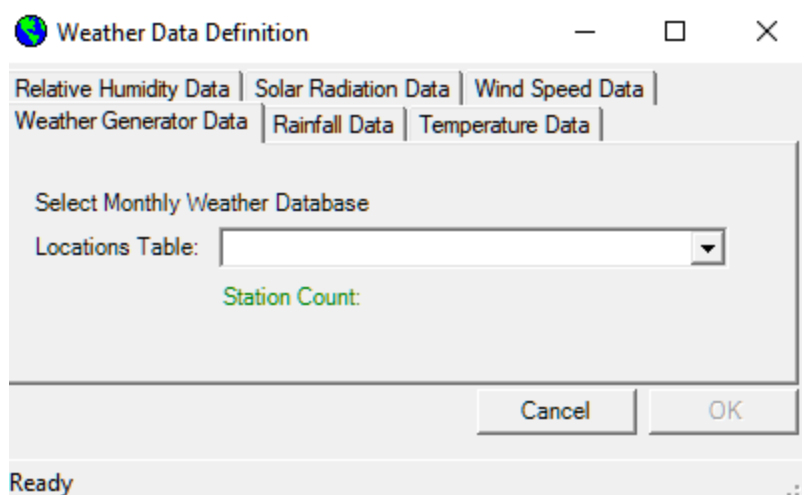


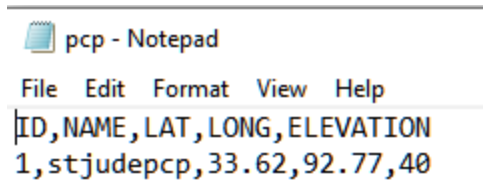
Figure 4.17 SWAT editor dialog box for defining the weather data

4.5.1.1 Rainfall Data

To input observed rainfall data multiple txt files, need to be created and saved within the SWAT editor folder for the watershed (see 4.5.5.1 and 4.6.1 for data collection). The first file is titled “pcp” (figure 4.18) and contains a header line and is followed by one line for each rainfall station. For this research, a maximum of one station was used, therefore all “pcp” files were two lines total.

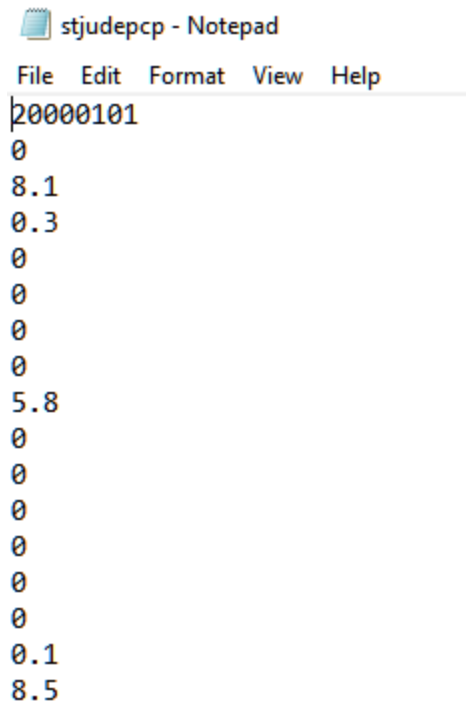
The first containing the titles “ID,NAME,LAT,LONG,ELEVATION.” The following lines consisted for the information of each rainfall station that coordinated with the title separated by a comma. The ID number started with “1” and the NAME was the name of the txt file that contained the observed data (described next). This “pcp” file is the file that is chosen in the “Location Table” within SWAT Editor.

A following txt file will need to be created for each rainfall station used. The format for the file is a first line with the start date in the format “YYYYMMDD” followed by a new data point on each line in mm (figure 4.19). This can be done in a time step of daily or sub-daily.



```
pcp - Notepad
File Edit Format View Help
ID,NAME,LAT, LONG,ELEVATION
1,stjudepcp,33.62,92.77,40
```

Figure 4.18: *pcp.txt* example



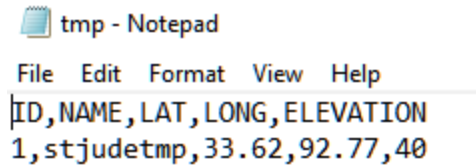
```
stjudepcp - Notepad
File Edit Format View Help
20000101
0
8.1
0.3
0
0
0
0
5.8
0
0
0
0
0
0
0.1
8.5
```

Figure 4.19: *pcp data.txt* example

4.5.1.2 Temperature Data

Temperature data is created in a similar way to rainfall data (see 4.6.2 for data collection). Instead of a “pcp” txt file being created a “tmp” file is created (figure 4.20). The “tmp” file is in the same format as the “pcp” file and again is the one chosen for the “Locations Table” within SWAT Editor.

The subsequent txt files with data are again in a similar format. The data is at the top and the data follows as one line per day of data. The unit of temperature data is degree Celsius and contains two column, one for daily low and the second column for daily-high (figure 4.21).

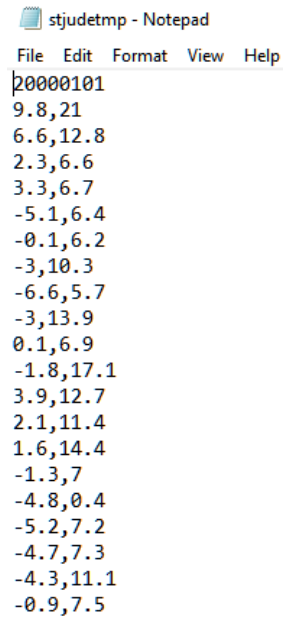


```

tmp - Notepad
File Edit Format View Help
ID, NAME, LAT, LONG, ELEVATION
1, stjudetmp, 33.62, 92.77, 40

```

Figure 4.20: tmp.txt example



```

stjudetmp - Notepad
File Edit Format View Help
20000101
9.8, 21
6.6, 12.8
2.3, 6.6
3.3, 6.7
-5.1, 6.4
-0.1, 6.2
-3, 10.3
-6.6, 5.7
-3, 13.9
0.1, 6.9
-1.8, 17.1
3.9, 12.7
2.1, 11.4
1.6, 14.4
-1.3, 7
-4.8, 0.4
-5.2, 7.2
-4.7, 7.3
-4.3, 11.1
-0.9, 7.5

```

Figure 4.21: tmp data.txt example

4.5.2 Writing Input Tables

Once all weather data is specified, the input files can be written to the SWAT database table by using the write SWAT Database Table dialog box and clicking “Select All” followed by “Create Tables”. If only one table needs to be created due to a change in the table, only that input file is checked and run to update the selected table (figure 4.22).

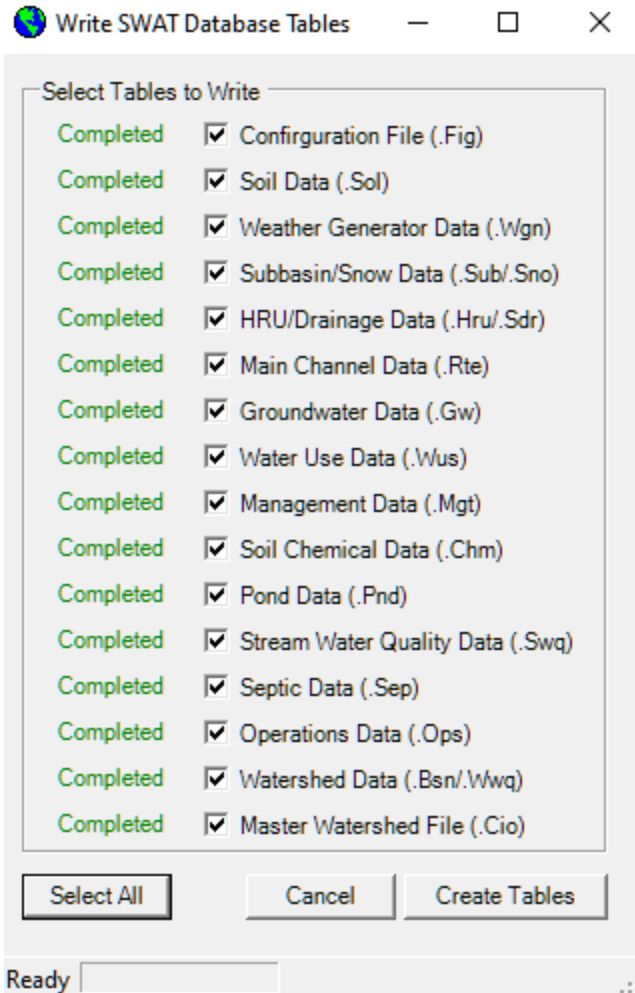


Figure 4.22: Dialog box for Write SWAT Database Tables

4.5.3 SWAT Simulation

Once all changes to the SWAT inputs have been made the, SWAT model is ready to run (figure 4.23). Under the Run SWAT tab, the starting and ending date were selected as well as the daily printout setting. The appropriate number of skip years for each run were chosen in the NYSKIP box. Next, “Setup SWAT Run” was chosen and once complete the SWAT model was run by clicking the “Run SWAT” box.

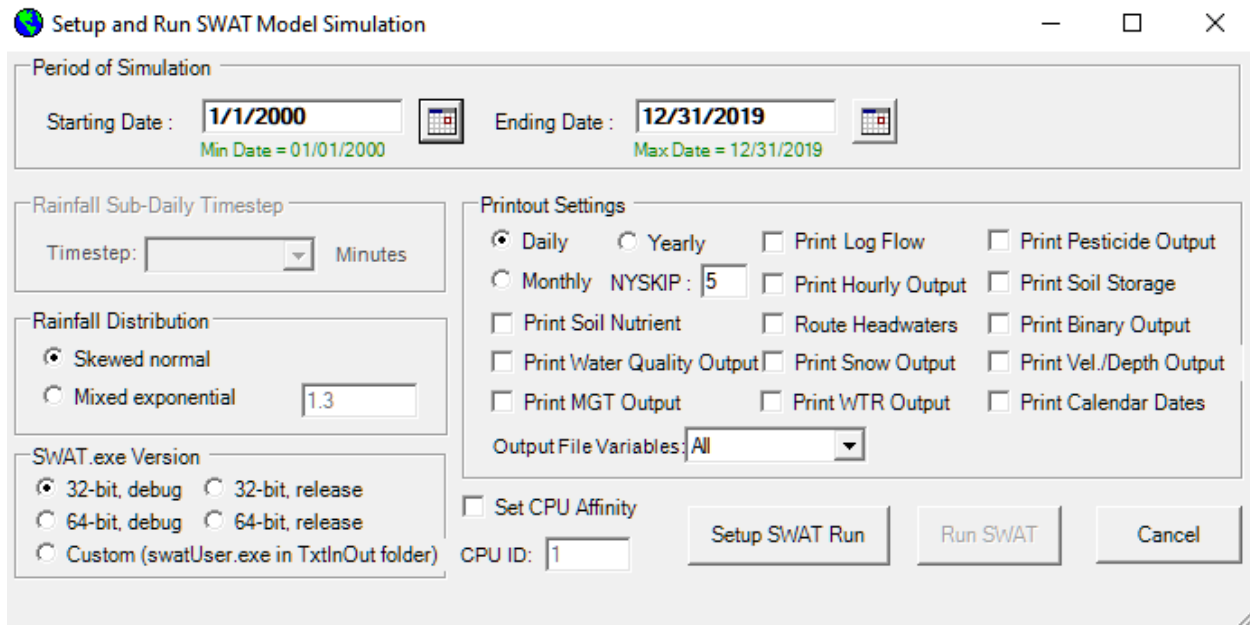


Figure 4.23: Swat editor dialog box for Setingup and Running SWAT Model Simulator

Going to “Read SWAT Output” allowed for SWAT simulations to be saved by clicking the output files to input (for this research output.rch was used), clicking the “Import Files to Database”, and then saving the simulation under a unique name (figure 4.24).

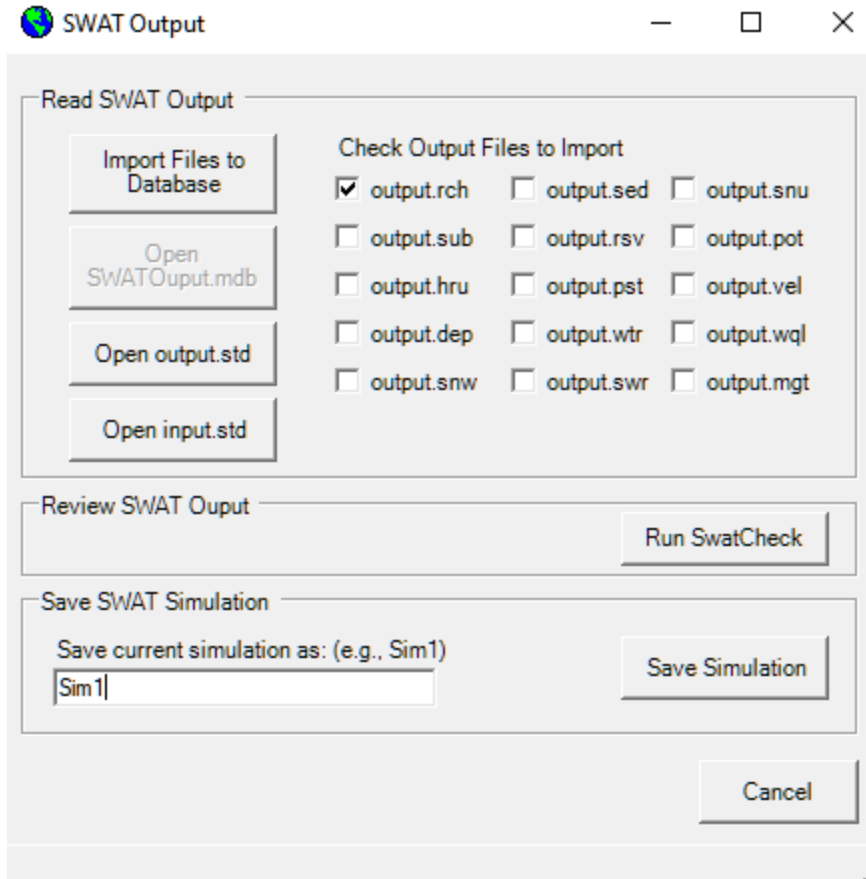


Figure 4.24: SWAT output menu

4.5.4 Calibration

A calibration and validation process allows for a studied subbasin to be an accurate reflection of the studied basin (Arnold et al., 2012b). This is done through a variety of steps, the first being a sensitivity analysis. The goal of a sensitivity analysis is to determine which parameters are the most sensitive to the particular subbasin and model being studied (Arnold et al., 2012b). This is done by changing a variety of parameters and comparing the outputs. This can either be done through a local sensitivity analysis or a global sensitivity analysis. A local sensitivity analysis changes parameters one at a time to determine which ones cause output values to change the most (Arnold et al., 2012b). Global sensitivity analysis is done by changing all parameters at once. Global sensitivity analysis require a lot more simulations to determine

the most sensitive parameters, however, local sensitivity analysis does not take into account how one parameter can affect other parameters (Arnold et al., 2012b).

Once the parameters are chosen calibration can begin. For calibration a set of local observed data is needed such as streamflow, evapotranspiration, or groundwater flow. This observed data is then compared with the model output data and parameters are changed until simulated data accurately represents the observed data (see 4.4.3). This is done through the final step: validation (Arnold et al., 2012b). The validation process ensures that the model can produce an accurate simulation of the studied component. It is done by comparing the model to data not used in the calibration process. This calibration and validation process can be done either manually or with an auto calibration tool (Arnold et al., 2012b). Manual calibration can be difficult especially if many different parameters are changed. Auto calibration allows for a large amount of parameter values to be run.

4.5.5 Calibration Data

For the calibration to run, observed information must be utilized. For the studied subbasin, the observed information for the model included the precipitation and the flow rate.

4.5.5.1 Observed Precipitation

Correct observed precipitation is very important in having an accurate calibrated model (Daughtry, 2012). The observed precipitations for the calibration of the watersheds were taken from the national center for environmental information (NCEE) which is in connection with the national oceanic and atmospheric administration (NOAA) (figure 4.25). The station number for subbasin 07363500 was USC00033862 and was named KEO with a latitude, longitude of (34.603, -91.99). A small amount of data points that were missing were replaced with a value of

“0” as this was the most common value. These years were chosen due to availability of not only the precipitation but also the observed-out flow.

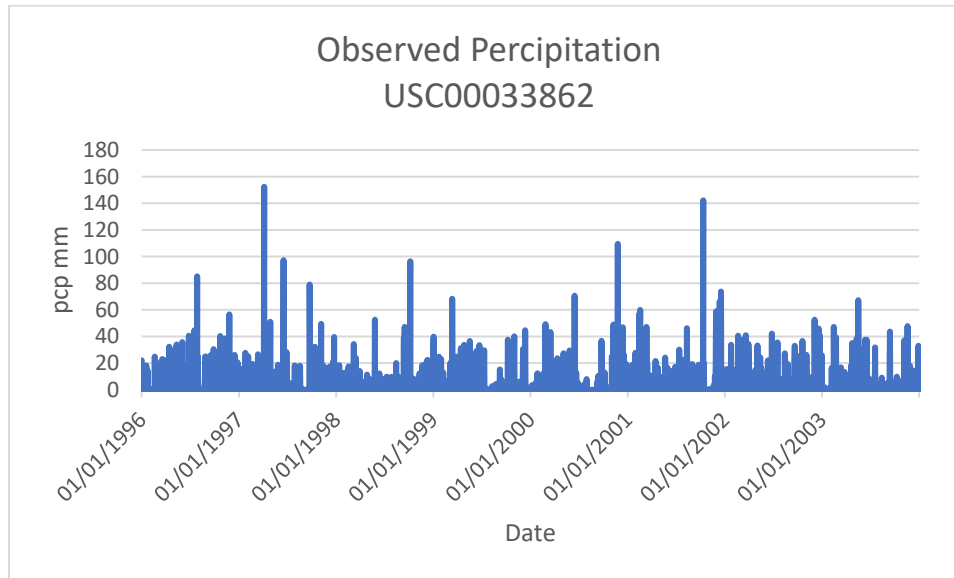


Figure 4.25: Precipitation in mm for daily data from January 1, 1996 to December 31, 2003 for USC site number 00033862. <https://www.ncdc.noaa.gov/cdo-web/search>.

4.5.5.2 Observed Out Flow.

The observed outflow used for the calibration of the two watersheds were taken from the United States Geological Services (USGS) database. USGS has outflow monitors at the outlet of many subbasins. For the subbasin in this study, the flow rate was taken from 1996-2003 (Saline River, USGS) (Figure 4.26). This gauging station was selected as it represents the response of the modeled subbasin most closely. The years were chosen based on availability of not only the flow rate but also the rainfall. Any missing daily data was replaced with the last given flow rate. This date range was chosen due to its minimal missing data. The data was given in cubic meters per second (cms).

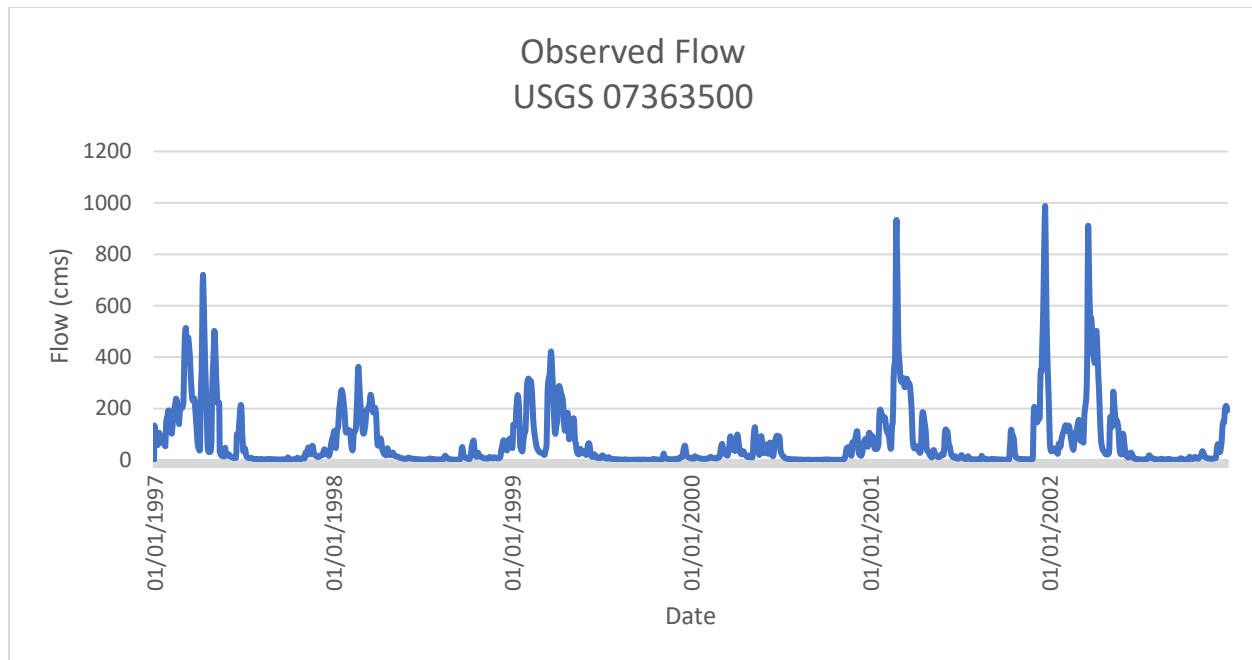


Figure 4.26 Average daily flow rate in cubic meters per second (cms) from January 1, 1997 to December 31, 2002, at USGS site number 07363500. <https://waterdata.usgs.gov/monitoring-location/07363500/#parameterCode=00065&period=P7D>.

4.6 SWAT Cup

For this study, SWAT-CUP (calibration and uncertainty program) was used as an auto calibration tool. It uses the Sequential Uncertainty Fitting algorithm (SUFI2) to calibrate the model (Abbaspour, 2012).

4.6.1 Sensitivity Analysis

For the public version of SWAT-CUP, only four parameters can be selected for calibration. The selected parameters for this study are the runoff curve number (cn2), baseflow alpha factor (ALPHA_BF) in units 1/days, groundwater delay time (GW_DELAY) in units days, and the deep percolation (GWQMN) in mm of water (Arnold et al., 2012a). These parameters were used for this study due to previous research (Ashine and Bedane, 2022) and can be seen in Table 4.2.

Parameter	Method	Minimum Value	Maximum Value
cn2	Relative	-0.2	0.2
Alpha	Replace	0	1
GW_DELAY	Replace	30	450
GWQMN	Replace	0	2

Table 4.2: Parameter change method maximum and minimum values for calibration

HRU	cn2 climate	cn2 100FRST	cn2 1/3 URBN	cn2 2/3 URBN	cn2 100 URBN	alpha (days)	gw_delay (days)	gwqmn (mm)
1	65.8228	65.8228	98	65.8228	65.8228	0.623	160.62	1.026
2	65.8228	65.8228	98	65.8228	65.8228	0.623	160.62	1.026
3	65.8228	65.8228	98	65.8228	65.8228	0.632	160.62	1.026
4	65.8228	65.8228	98	65.8228	65.8228	0.623	160.62	1.026
5	58.324	60.8236	98	60.8236	59.9904	0.623	160.62	1.026
6	65.8228	65.8228	98	65.8228	65.8228	0.632	160.62	1.026
7	65.8228	65.8228	98	65.8228	65.8228	0.623	160.62	1.026
8	65.8228	65.8228	98	65.8228	65.8228	0.623	160.62	1.026
9	64.15639	65.8228	98	65.8228	65.8228	0.632	160.62	1.026
10	64.15639	65.8228	98	65.8228	65.8228	0.623	160.62	1.026
11	64.15639	65.8228	98	65.8228	65.8228	0.623	160.62	1.026

Table 4.3: HRU calibrated parameter values

4.6.2 SWAT Cup Setup

The calibration process utilized data from 1/1/1996 to 12/31/2002 again with a one-year warm up period so printing began at 1/1/1997.

The warm-up period, also known as the equilibration period is important especially for shorter simulation periods (Arnold et al., 2012a). This fully allows for the hydrologic cycle to become operational (Arnold et al., 2012a). A one-year period is normally acceptable (Arnold et

al., 2012b). In this study, a five-year warm up is used for model runs and a one year warm up is used for calibration runs due to a limited data of observed flow rates and precipitation.

An observed rch.txt as well as an observed.txt file was updated to include the observed data. This study had 11 subbasins, with the outflow point in subbasin 1 (figure 4.11).

4.6.3 Evaluation of Model performance using NSE metric

The calibration process gives many different outflow simulations, and a list of the best parameter values was printed. The best calibration was chosen by comparing the observed and simulated outflow rates for each of the given scenarios (Figure 4.27). The parameter values that produced an outflow rate with the highest observed Nash-Sutcliffe efficiency (NSE; Eqn 1). The NSE is determined using the following formula:

$$NSE = 1 - \frac{\sum_{i=1}^n (Observed_i - Simulated_i)^2}{\sum_{i=1}^n (Observed_i - Observed_{average})^2} \quad (Eqn 1)$$

There is no absolute threshold for a satisfactory NSE value (Gassman, 2007). While a value exceeding 0.5 is proposed to be a valid NSE (Moriassi et al., 2007), there are other arguments that any value between 0 and 1 are also considered a valid performance (Moriassi et al., 2007). Additionally, there are many studied that have a calibrated and/or validated monthly NSE less than 0.5 (Gassman, 2007; Afinowicz et al., 2005; Coffey et al., 2004; Du et al., 2005). The NSE received for a monthly time step for calibration was 0.51 (Figure 4.28) and for validation (see below) was 0.43 (Figure 4.29). Due to past research these NSEs can be concluded to be appropriate.

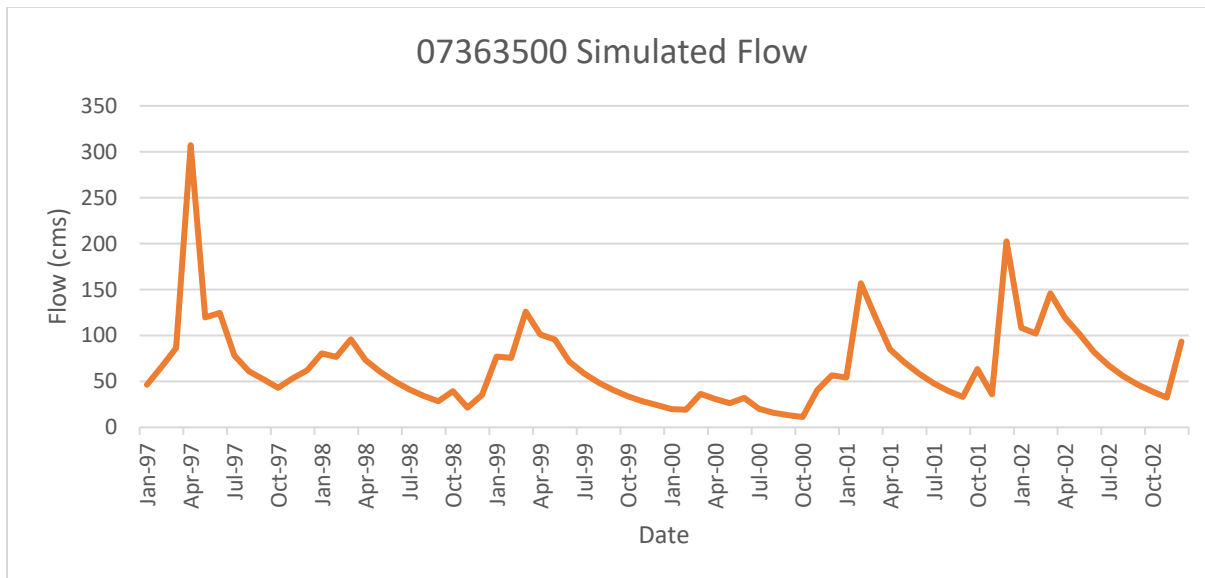


Figure 4.27 Simulated average monthly flow rate in cubic meters per second (cms) from January 1, 1997 to December 31, 2002 at the outlet of the river basin 007363500.

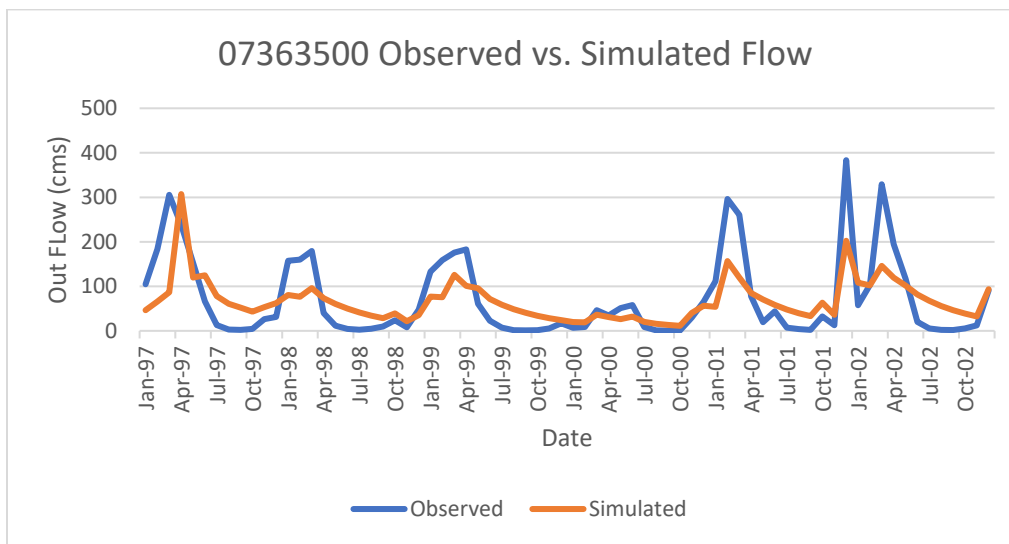


Figure 4.28 Observed and the simulated average monthly flow rate in cubic meters per second (cms) from January 1, 1997 to December 31, 2002 at river basin outlet (USGS ID 07363500)

The following change values for the parameters calibrated created the acceptable outflow:

Parameter	Method	Value
cn2	Relative	-0.1668
Alpha	Replace	0.6230
gw	Replace	160.6200
gwq	Replace	1.0260

Table 4.4: List of calibrated parameter value changes

4.6.4 Validation

Once calibration is complete the results must be validated. Using observed rainfall and the calibrated parameters, additional simulated data was collected and compared to observed data. An additional simulation year was run for the year 2003- a year that experience high, low, and medium flow- to determine a valid simulation (Arnold et al., 2012b). The NSE for this year was 0.43.

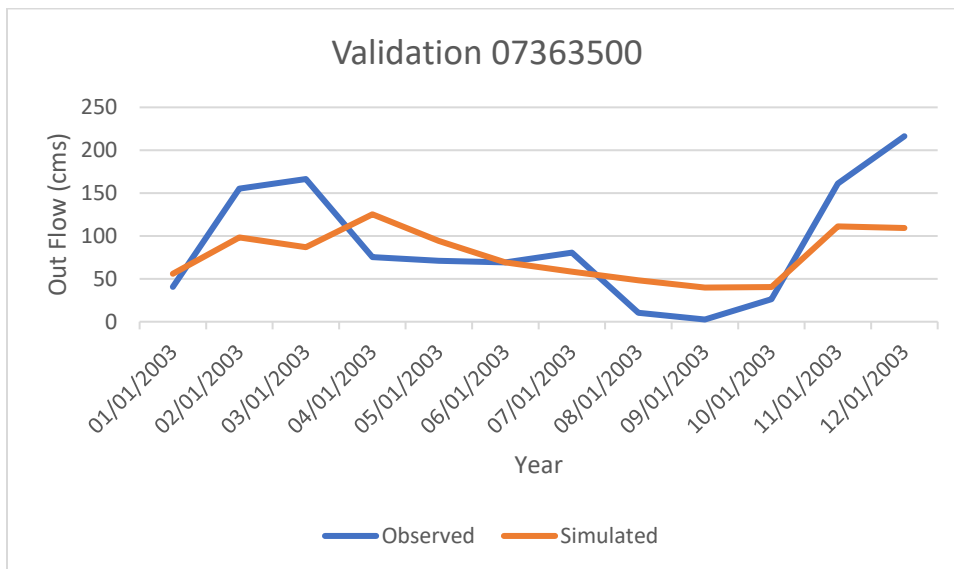


Figure 4.29 Line chart showing the simulated and observed flow during the validation period

4.7 Climate Change and Hydrological Response

One of the objectives of this study is to determine how the flow, groundwater flow, and evapotranspiration change due to projected climate change. To achieve this, the study gathered the projected rain fall and precipitation data for the two selected 20 year future period i.e., 2040 and 2080.

4.7.1 Future Climate Data

There are many climate models widely used to generate climate projection data for hydrological simulation. These are broadly classified into four types (Kour and Patel, 2016) namely: energy balance models, radiative convection models, statistical dynamic models, and global climate models.

Global climate models (GCMs) (Kour and Patel, 2016). GCMs are complex models that utilize physics fundamentals as well as greenhouse gas assumption levels to simulate the climate response (Kour and Patel, 2016). They are used heavily in projecting various aspect of future water resources. However, their complexity leads to many uncertainties (Kour and Patel, 2016). While they are able to create fairly accurate models on both the global and continental scale, more regional techniques have only appeared more recently (Kour and Patel, 2016).

The climate data used in this study was collected from MarkSim, a weather file generator website (MarkSim, <http://gisweb.ciat.cgiar.org/marksimgcm/>). MarkSim allows for longitude and latitude to collect data from a variety of models and RCP. For this experiment, a latitude and longitude close to our sites was chosen at 33.950, -91.671. All GCMs available were selected and the results were an average of the following models: BCC-CSM1-1, BCC-CSM1-1-M, CSIRO-Mk3-6-0, FIO_ESM, GRDL-CM3, GFDL-ESM2G, GFDL-ESM2M, GISS-E2-H, GISS-

E2-R, HadGem2-ES, IPSL-CM5A-LR, IPSL-CM5A-MR, MIROC-ESM, MIROC-ESM-CHEM, MIROC5, MRI-CGCM3, and NorESM1-M.

RCPs 2.6 and 8.5 were selected for both time periods 2040-2059 and 2080-2099. The daily high and low temperatures (Celsius) as well as rainfall (mm) was used for this objective. RCP 2.6 shows a high effort to curb emissions and minimize climate change, while RCP 8.5 represents a low effort to curb emissions and greater changes in climate. By the year 2070, RCP 2.6 calculates a net negative carbon dioxide emission making 2080-2099 data important to study (Climate Watch, unicef). RCPs 2.6 and 8.5 are the two extremes (one represent the mitigation scenario (2.6 watt/m² at the end of 21st century) and another represent the upper extreme warming scenarios 8.5 watt/m² at the end of 21st century chosen in this study to evaluate impact of future changes on different component of hydrological cycle.

4.7.2 Future projection using calibrated SWAT Model

Once the precipitation and rainfall were added to the model in SWAT Editor, the model was opened in SWAT-CUP. Here, the minimum and maximum for the four parameters were both set to the calibrated value. The streamflow, groundwater, and evapotranspiration were set up to be calculated at subbasin 1 of the watershed. This is the subbasin that contains the outflow point.

The streamflow was run with the output.rch file at subbasin 1. This measures the flow for the main reach of this subbasin which, since it is the outstreamflow subbasin accounts for all of the water in the watershed. However, the evapotranspiration and ground water streamflow cannot be calculated in this output file. Therefore, these two hydrological processes were printed to the output.sub file. This calculates the evapotranspiration and ground water streamflow occurring only in this subbasin.

SWAT divides ground water into a shallow system, which is streamflow that that will contribute to return flow, and a deep system, which does not have return flow (Arnold, Soil, 2012). The ground water studied (GW_Q) refers to the ground water (mm) that will enter the shallow aquafer (Arnold et al., 2012a).

The model was run with a 5-year warm up period. This was done 4 times and the data was collected from 2045-2059 for RCP 2.6 and 8.5 as well as from 2080-2099 for RCPs 2.6 and 8.5. Files were printed in a daily time step and converted to a monthly average. Therefore, the ground water and evapotranspiration is given in the units millimeters per day (mm/day) and the streamflow is measured in a consistent cubic meters per second (cms)

4.7.3 USACE's Climate Hydrology Assessment

USACE's Climate Hydrology Assessment Tool can be used to compare to the flow rate data collected. Note that climate Hydrology Assessment does not use simulation with RCP 2.6 (mitigation scenario) and only provide projection corresponding to RCP 4.5 and RCP 8.5 (figure 4.30). This figure can help to better understand the results given as well as confirm the accuracy of such results.

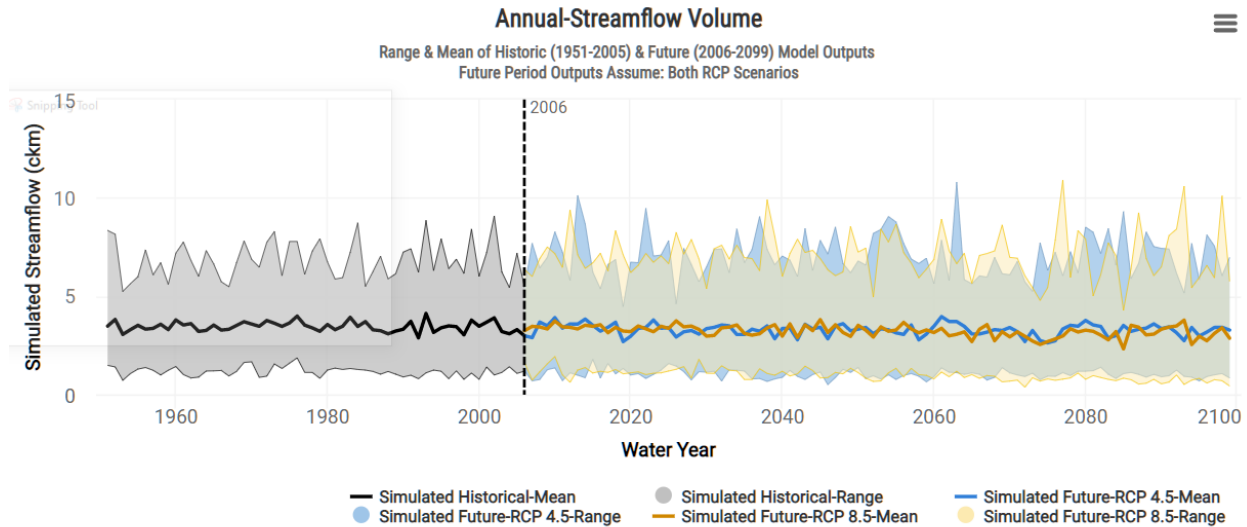


Figure 4.30: Simulated Annual-streamflow volume at the watershed scale from the past 1950s until 2100 The shaded region shows the spread in projection among climate models This image was created using USACE's Climate Hydrology Assessment Tool founded on the website: <https://climate.sec.usace.army.mil/chat/>.

4.8 Land use and Hydrological Response

In order to achieve objective 2, the SWAT model was run with synthetic land use scenarios.

4.8.1 Land Use Data

In order to determine how land use influenced hydrological processes, the land use look up tables in the QSWAT set up were changed in order to get a varying degree of URBN land use. Land use data was changed to increase roughly 1/3 in URBN per run until 100% URBN land use was reached.

Subbasin 07363500 first had a 100% FRST run followed by a 30.98% URBN and 69.02% FRST (1/3 URBN) run. Next was a 69.02% URBN and 30.98% FRST run (2/3 URBN) and a 100% URBN run.

4.8.2 Hydrological simulation of SWAT Model

Once the land use data was updated in QSWAT, precipitation and temperature data was added in SWAT Editor. Data from 2040 with an RCP of 2.6 was used for all runs. The SWAT model was then run in the same way as section 4.7.2.

Chapter 5: Results and Discussion

5.1 Climate Change and Hydrological Response

The first objective of this study was to determine how temperature and rainfall climate change projections would impact streamflow rate, evapotranspiration, and groundwater flow. This objective was completed by using data for RCP 2.6 and 8.5. In addition, two time periods were studied. 2040 data was taken from the year 2040-2059, though with a 5-year warm up period, data shown is from the year 2045-2059. 2080 data has the same 5-year warm up period and data shown is from the years 2085-2099. The time period 2045-2059 is defined as 2040. The time period 2085-2099 is defined as 2080.

Figure 4.29 shows the USACE's annual streamflow value simulated with projection from RCP 4.5 and RCP 8.6 (Climate Hydrology Assessment, USACE). As seen below, the flow results of this study closely correlate with the simulation from the Climate hydrology assessment of USACE. Results also show that the flow rate will decrease from the year 2040 to 2100, especially for simulation run with extreme RCP 8.5 scenarios.

		2040		2080	
		RCP 2.6	RCP 8.5	RCP 2.6	RCP 8.5
Flow (cms)	average	108.89	109.61	109.65	100.49
	maximum	311.36	311.09	302.62	330.32
	minimum	23.67	23.50	20.73	17.43
	standard				
	deviation	58.12	58.20	57.74	51.62
Evapotranspiration (mm/day)	average	2.10	2.13	2.11	2.21
	maximum	4.26	4.35	4.59	4.52
	minimum	0.46	0.49	0.48	0.49
	standard				
	deviation	1.00	1.01	1.00	1.07
Groundwater (mm/day)	average	1.38	1.38	1.39	1.27
	maximum	3.19	3.24	3.25	3.12
	minimum	0.36	0.36	0.26	0.29
	standard				
	deviation	0.54	0.54	0.56	0.49

Table 5.1: Model Simulation Summery of flow, evapotranspiration, and groundwater for 2040 and 2080 period

5.1.1 Model Response to RCP 2.6 vs 8.5

RCPs 2.6 and 8.5 were compared for the data set starting in the year 2040 and starting in the year 2080.

5.1.1.1 Model Simulation for 2040 Period

Data was collected starting in the year 2040. A five-year warm up period was implemented, and data was printed from the years 2045-2059.

5.1.1.1.1 Streamflow

Figure 5.1 shows how the monthly average streamflow rate in 2045-2059 differs with an RCP of 8.4 and RCP of 2.6. As seen in the figures, there is not much difference over the 15 years between the two scenarios. Table 5.1 shows how both subbasins studied have similar average, maximum, minimum, and standard deviation numbers with all values within 1 cms. RCP 8.5 has a higher average streamflow rate and standard deviation but a lower maximum and minimum monthly flow rate than RCP 2.6.

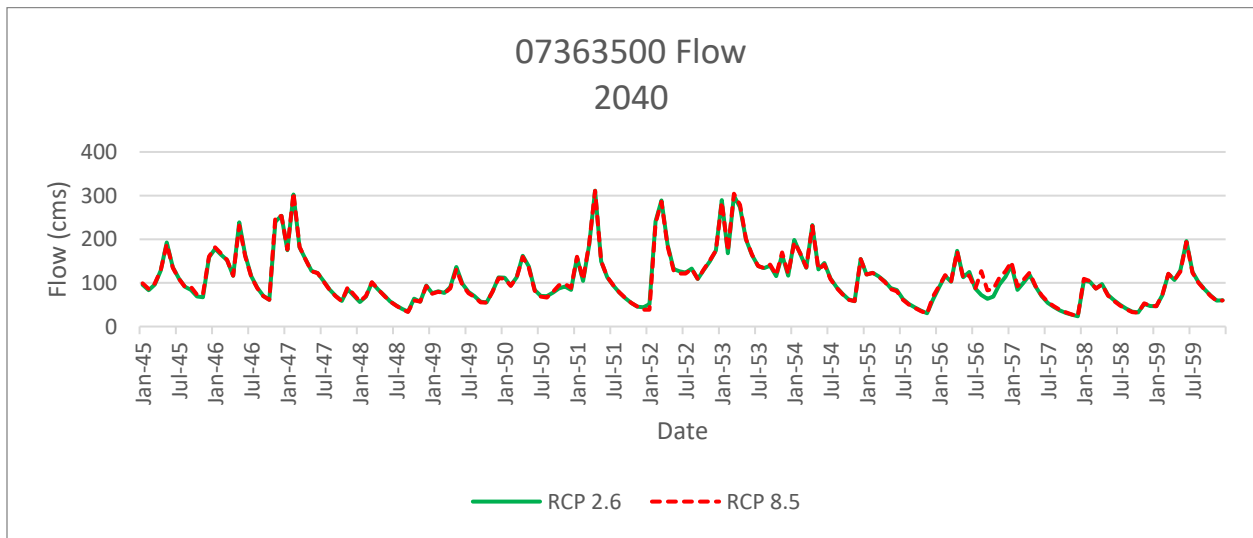


Figure 5.1 Monthly average flow in cubic meters per second for river basin 07363500 from years 2045 – 2059 for both RCP 2.6 and RCP 8.5 scenario.

5.1.1.1.2 Evapotranspiration

Figures 5.2 shows the monthly average evapotranspiration from the years 2045 to 2059 in millimeters per day (mm/day). Similarly, to the streamflow rate, there is very little difference seen between the two different RCPs on the graphs. Table 5.1 again confirms this as the

average, maximum, minimum, and standard deviation between data sets 2.6 and 8.5 are all less than or equal to 0.09 mm/day (subbasin 07363500).

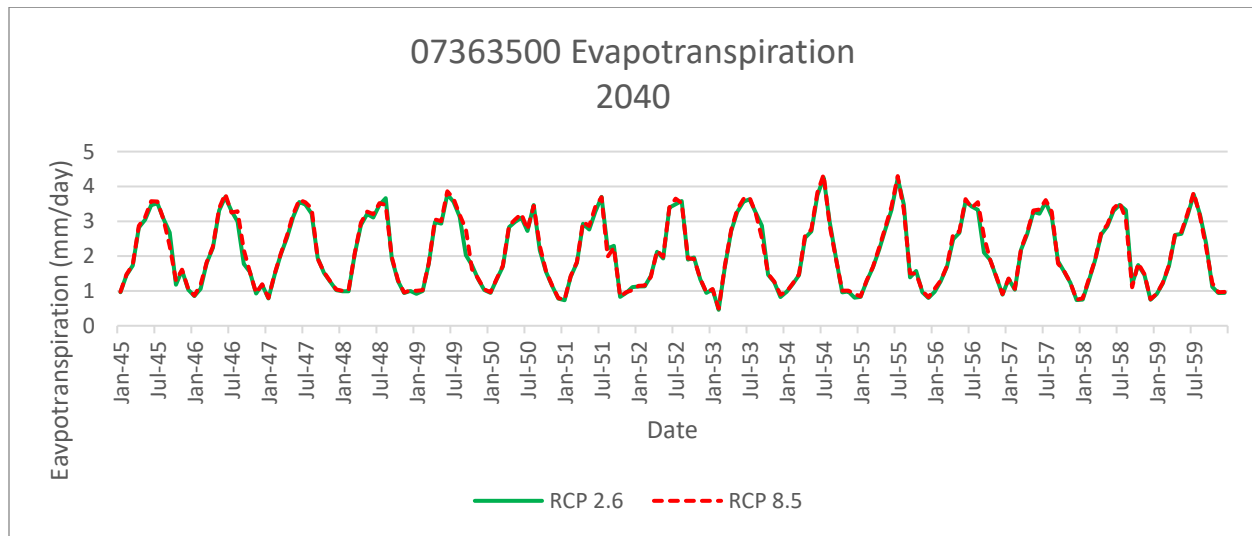


Figure 5.2 Monthly average evapotranspiration in millimeters per day for river basin 07363500 from years 2045 – 2059 for both RCP of 2.6 and 8.5.

5.1.1.1.3 Groundwater

Figure 5.3 shows how the monthly average groundwater flow (measured in mm/day) varies with RCP 2.6 and 8.5 for the years 2045 to 2059. Like the previous two hydrological processes studied, little difference is seen between the data sets. Again, this is further seen through Table 5.1 in which the difference in average, maximum, minimum, and standard deviation is less than or equal 0.05 mm/day.

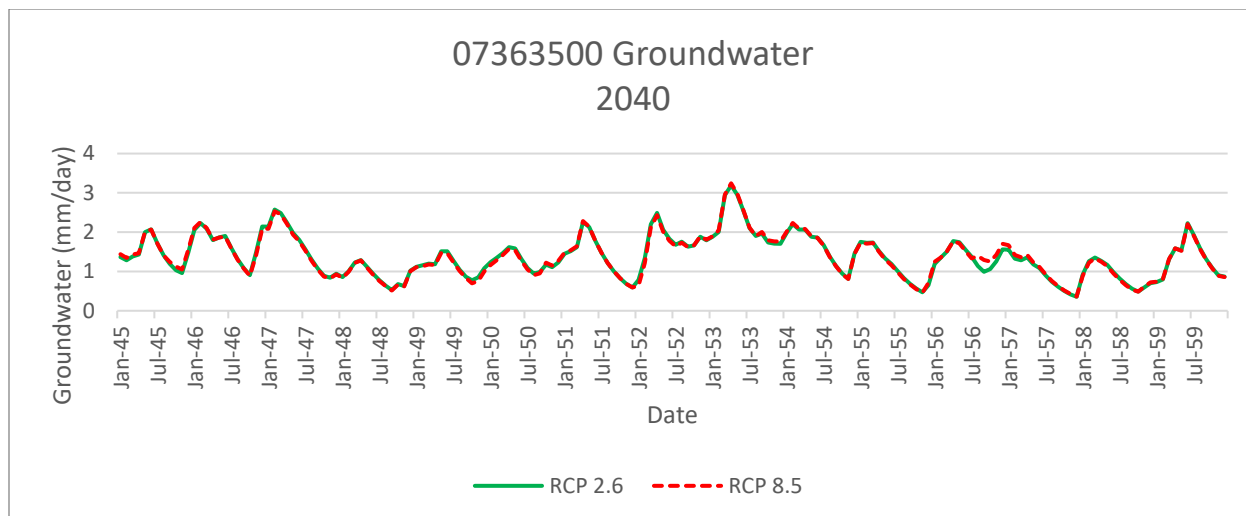


Figure 5.3 Monthly average groundwater flow in millimeters per day for subbasin 07362000 from years 2045 – 2059 for both RCP2.6 and RCP 8.5.

5.1.1.2 Model Simulation for 2080 Period

Data was collected starting in the year 2080. A five-year warm up period was used for all hydrological simulation, and simulation data for the years 2085-2099 was used for analysis.

5.1.1.2.1 Streamflow

Figure 5.4 shows how the monthly average streamflow rate in 2085-2099 differs with an RCP of 8.4 and RCP of 2.6. These two figures show a more variability than the figures for the 2040 data set (Figures 5.1 and 5.2). Both the figures show RCP 2.6 averaging higher streamflow rates than RCP 8.5.

This is supported by Table 5.1 which concludes a higher average streamflow rate by 14.21cms for subbasin 07362000 and 9.16cms higher for subbasin 07363500. However, the maximum monthly average streamflow rate was found in the RCP 8.5 data set and was 27.7cms higher than RCP 2.6. Additionally, a lower minimum value is reported for RCP 8.5. Finally, the standard deviation for RCP 2.6 is higher than RCP 8.5 (by 6.12cms) showing that RCP 2.6 data has more variability in its streamflow rates.

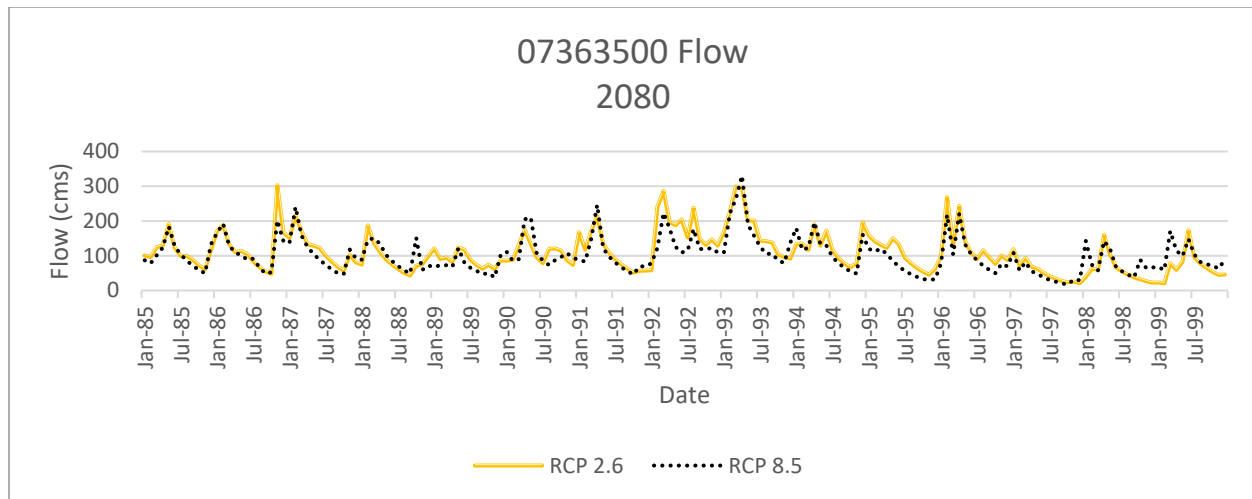


Figure 5.4 Monthly average flow in cubic meters per second for subbasin 07363500 from years 2085 – 2099 for both RCP 2.6 and RCP 8.5.

5.1.1.2.2 Evapotranspiration

Figures 5.5 shows the monthly average evapotranspiration from the years 2085 to 2099 in millimeters per day (mm/day). This figure shows similar shapes in evapotranspiration with slightly higher peaks for RCP 8.5.

Table 5.1 supports this by showing a slightly higher average evapotranspiration for RCP 8.5 for both subbasins. The maximum monthly average for both subbasins is found in the RCP 2.6 data set for subbasins as well as the lowest minimum streamflow rate. RCP 8.5 has more variability in evapotranspiration with slightly higher standard deviations. However, the maximum, minimum, and standard deviation values between RCPs 2.6 and 8.5 are less than 0.1 mm making these differences very slight.

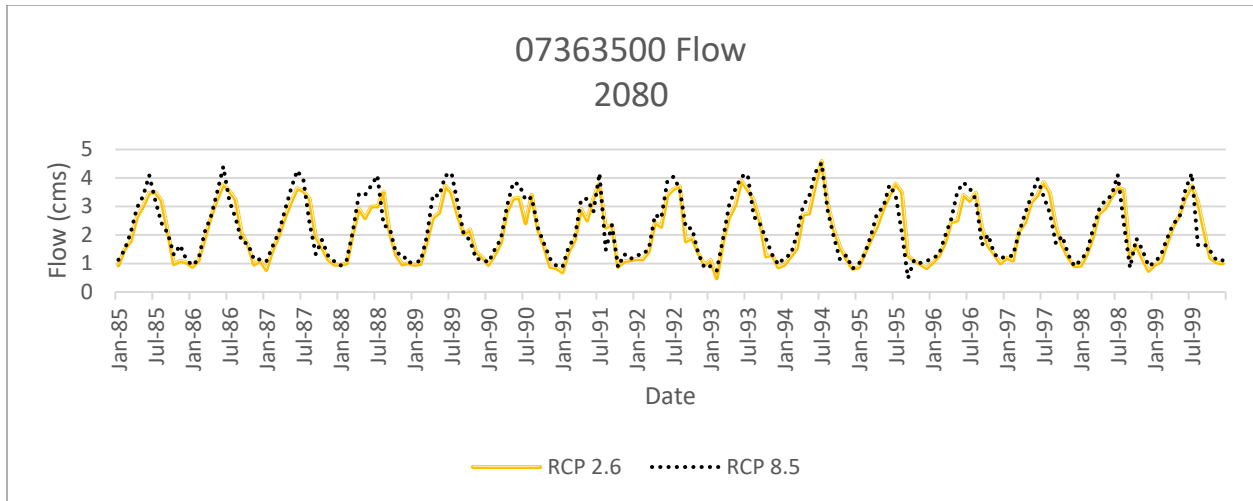


Figure 5.5 Monthly average evapotranspiration in millimeters per day for subbasin 07363500 from years 2085 – 2099 for both RCP 2.6 and RCP 8.5.

5.1.1.2.3 Groundwater

Figure 5.6 shows the monthly average groundwater flow from the years 2085 to 2099 in mm/day. The results show a similar shape for both RCPs but with RCP 8.5 being lower than RCP 2.6. This is confirmed in Table 5.1 where the average groundwater flow is higher for RCP 2.6 by 0.12 mm/day. Additionally, RCP 2.6 has a higher maximum, lower minimum, and higher standard deviation than RCP 8.5.

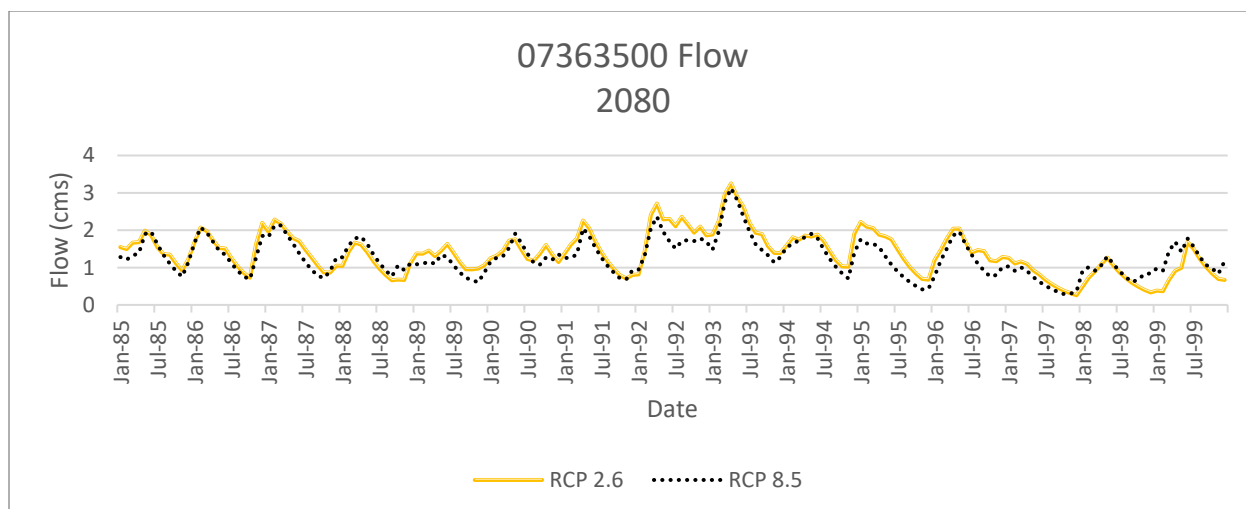


Figure 5.6 Monthly average groundwater flow in millimeters per day for subbasin 07362000 from years 2085 – 2099 for both RCP 2.6 and RCP 8.5.

5.2 Hydrological Simulation: Future periods (2040s and 2080s)

Model simulation two data period i.e., 2040 (2045-2099) and 2080 (2085-2099) were used to analyse how the streamflow, evapotranspiration, and groundwater simulation are different in the two selected time periods.

5.1.2.1 Comparisons for RCP 2.6

Hydrological simulation run with RCP 2.6 projection data for two data period was used for comparative analysis i.e., 2040s and 2080s.

5.1.2.1.1 Streamflow at the basin outlet

Figure 5.7 shows the variations of streamflow for years 2045-2059 and 2085-2099 with an RCP 2.6. While the simulation shows a lot of variability in flow, Table 5.1 shows that the values for the data period are very similar. The difference between the average streamflow is less than 1 cms.

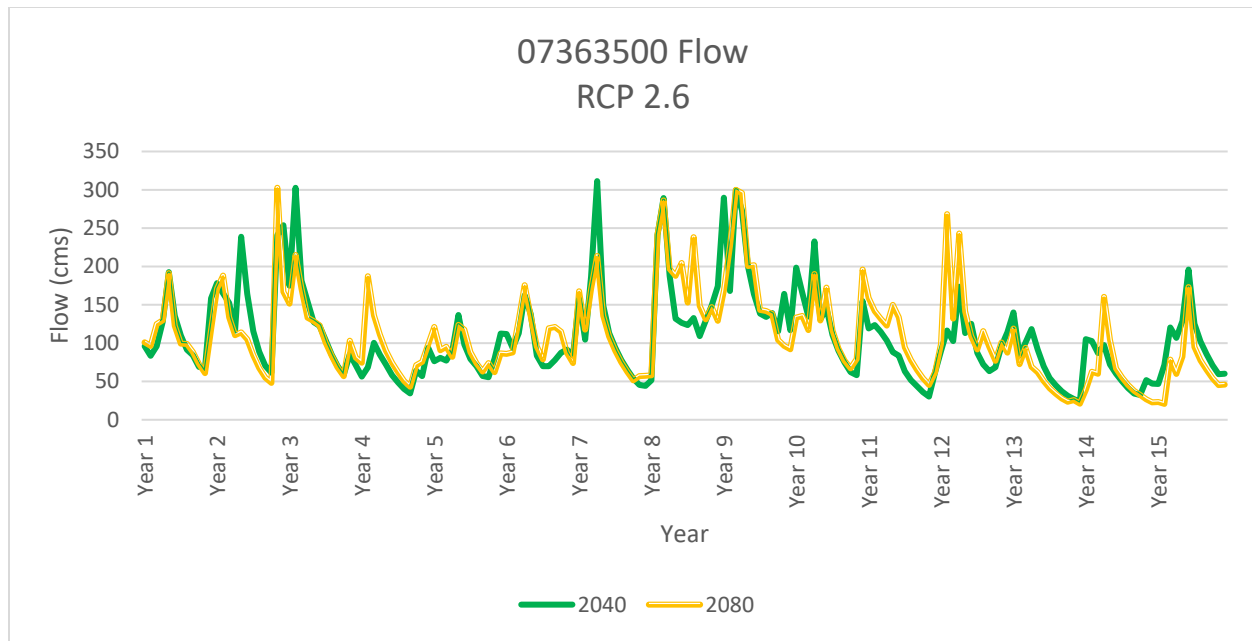


Figure 5.7 Monthly average flow in cubic meters per second for subbasin 07363500 with RCP 2.6 from year 1 (2045 for 2040 data and 2085 for 2080 data) through year 15 (2059 for 2040 data and 2099 for 2080 data)

5.1.2.1.2 Evapotranspiration

As seen in figure 5.8, the evapotranspiration for years 2040 and 2080 with a RCP 2.6 are very similar. This can be further seen in Table 5.1 where, the average evapotranspiration is 0.01mm/day apart and the standard deviations for 2040 and 2080 have the same values. The maximum (for the 15 year simulation period) and minimum (for the 15 year simulation period) evaporation are also similar..

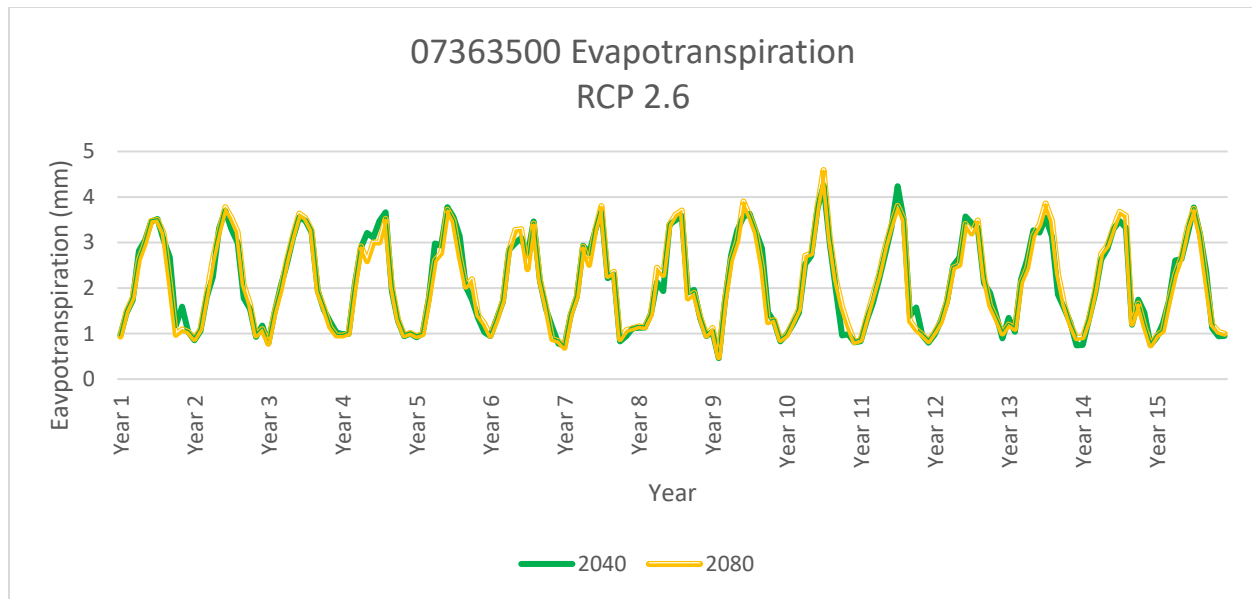


Figure 5.8 Monthly average evapotranspiration in millimeters per day for subbasin 07363500 with RCP 2.6 from year 1 (2045 for 2040 data and 2085 for 2080 data) through year 15 (2059 for 2040 data and 2099 for 2080 data).

5.1.2.1.3 Groundwater

Similarly, to the the groundwater flow, for the two simulation periods are shown in figure 5.9. Groundwater flow simulation for both period are similar (See also Table 5.1) The results show that there are very similar values of average flow rate.

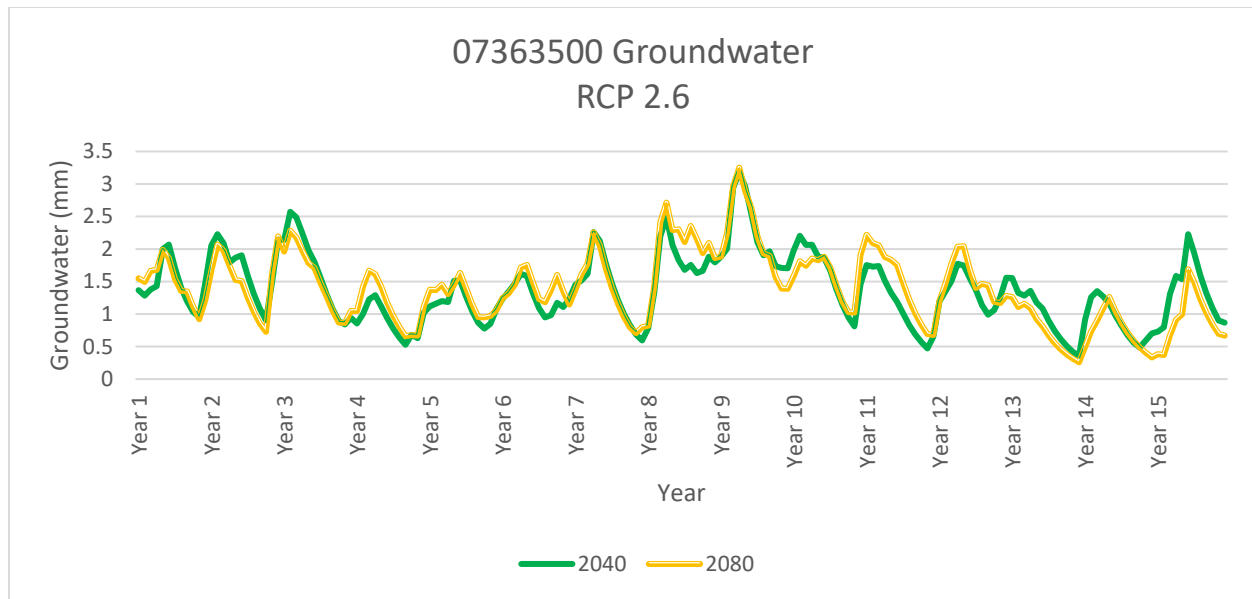


Figure 5.9 Monthly average groundwater in millimeters per day for subbasin 07363500 with RCP 2.6 from year 1 (2045 for 2040 data and 2085 for 2080 data) through year 15 (2059 for 2040 data and 2099 for 2080 data).

5.1.2.2 Hydrological response simulated with RCP 8.5

Different component of hydrological cycle simulated with SWAT forced with climate data from RCP 8.5 for two time periods (starting in the years 2040 and 2080) were analyzed.

5.1.2.2.1 Streamflow

Figure 5.10 show the comparison between the projected simulated flow with an RCP 8.5 for years 2045-2059 and 2085-2099. The flow peak for the 2080s period is smaller in magnitude to that of the 2040s (also see Table 5.1).

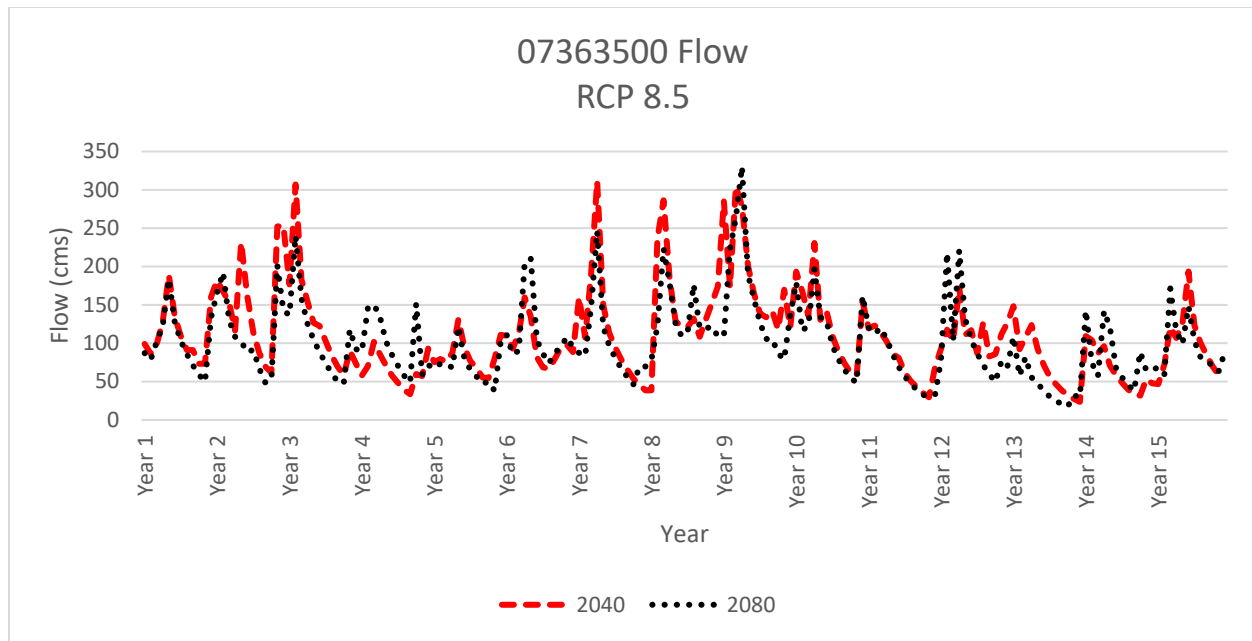


Figure 5.10 Monthly average groundwater flow in cubic meters per second for subbasin 07363500 with RCP 8.5 from year 1 (2045 for 2040 data and 2085 for 2080 data) through year 15 (2059 for 2040 data and 2099 for 2080 data).

5.1.2.2.2 Evapotranspiration

Figure 5.11 shows the simulated actual evapotranspiration in mm/day with an RCP of 8.5 for the two time periods i.e., 2040 and 2080. While differences in simulated values for the two periods are similar, the evapotranspiration for 2080s had higher peaks. Table 5.1 also shows that the simulated evapotranspiration for 2080s is comparatively higher than the 2040s period. For RCP 8.5 and for later time periods, more water is evaporated due to increase in potential demand with temperature.

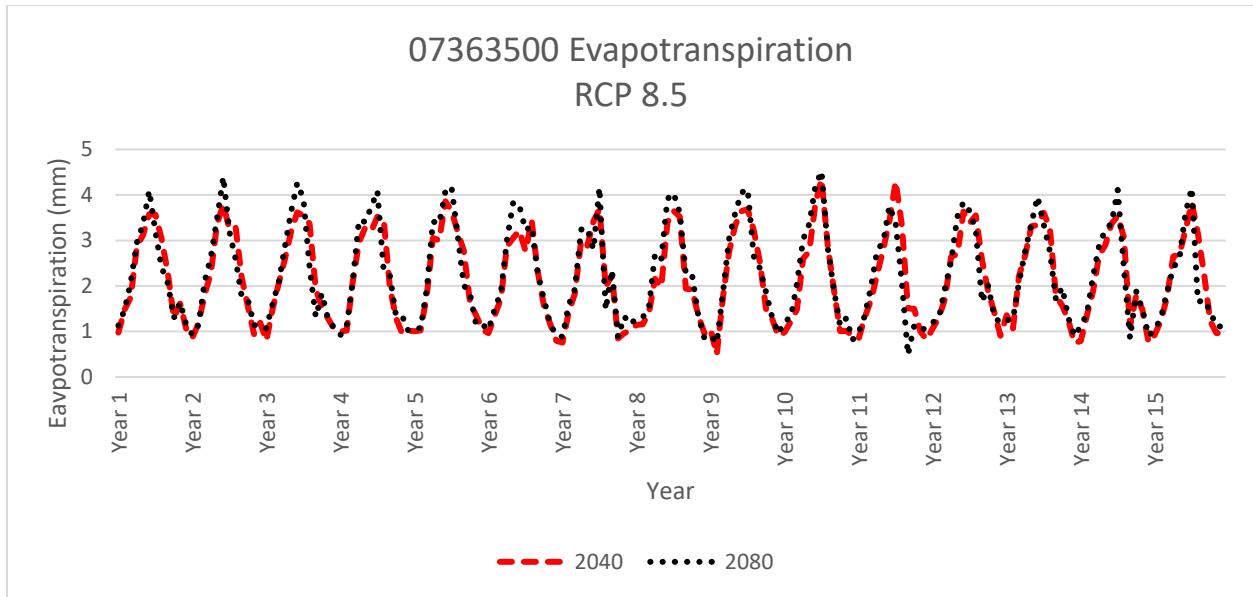


Figure 5.11 Monthly average evapotranspiration in millimeters per day for subbasin 07363500 with RCP 8.5 from year 1 (2045 for 2040 data and 2085 for 2080 data) through year 15 (2059 for 2040 data and 2099 for 2080 data).

5.1.2.2.3 Groundwater flow

Figure 5.12 shows the model simulated groundwater flow with an RCP 8.5 for the same two data periods 2040s and 2080s. As seen in the graph, and supported by Table 5.1, the simulated groundwater flow for the year 2040 is comparatively higher.

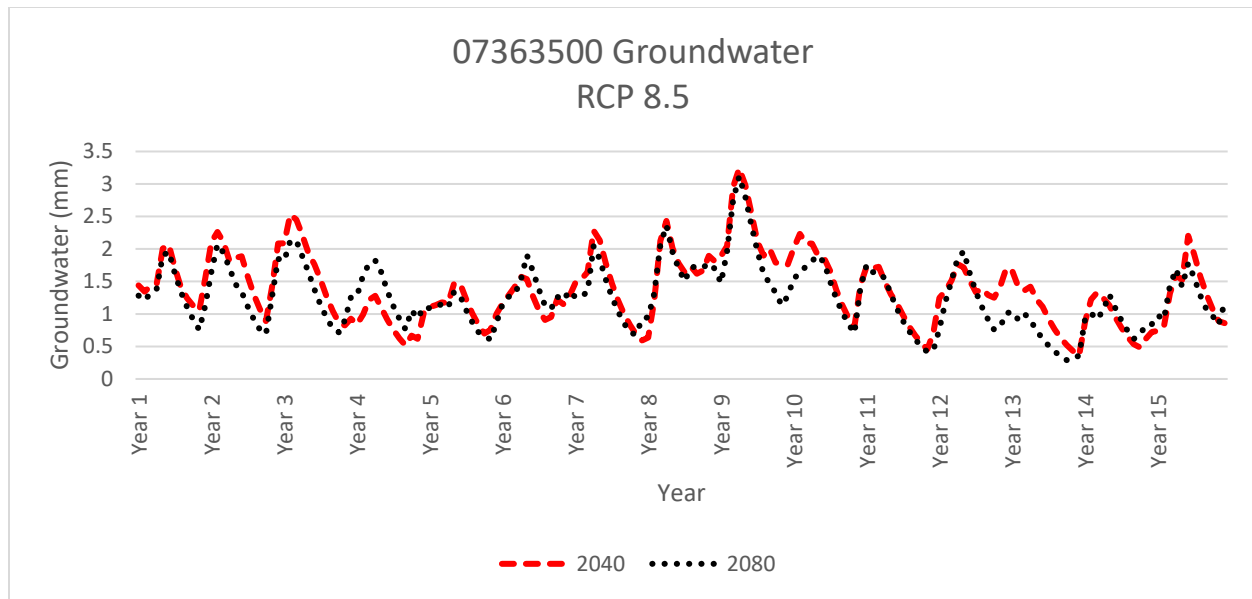


Figure 5.12 Monthly average groundwater in millimeters per day for subbasin 07363500 with RCP 8.5 year 1 (2045 for 2040 data and 2085 for 2080 data) through year 15 (2059 for 2040 data and 2099 for 2080 data).

5.2 Hydrological Simulation: Land Use Change

A second objective of this study was to determine how urbanization would impact streamflow rate, evapotranspiration, and groundwater flow. This objective was completed by updating the land use data. Four different synthetic land use maps were constructed for the experiment. The first land use map consisted of 100% of FRST land use type, the second had 1/3 of the total FRST were converted into URBN and remaining 2/3 as FRST. In the third scenario, the URBN class was further increased to 2/3 of the total area and remaining 1/3 was used as FRST, and the fourth synthetic land use comprised of 100% of URBN land use class. The projected (RCP 2.6) precipitation and temperature data from 2040s was used for this experiment. Note that a 5-year warm up was utilized, therefore the model simulation data from 2045-2059 was only used for comparative analysis..

		100% FRST	1/3 URBN	2/3 URBN	100% URBN
Flow (cms)	average	109.81	111.33	111.36	112.88
	maximum	314.03	333.98	387.26	420.15
	minimum	23.83	23.21	18.54	15.73
	standard deviation	58.44	62.51	73.10	79.35
Evapotranspiration (mm/day)	average	2.10			2.05
	maximum	4.26			5.27
	minimum	0.46			0.46
	standard deviation	1.00			1.18
Groundwater (mm/day)	average	1.38			0.54
	maximum	3.19			1.53
	minimum	0.36			0.09
	standard deviation	0.54			0.28

Table 5.2: Summary of hydrological simulation with synthetic land use scenario for Saline River Basin.

5.2.1 Simulated Streamflow

Figure 5.13 shows the streamflow rates (cms) of river basin with a land use of 100% Forest (FRST) and 100% urban (URBN). These comparison show that the streamflow for completely URBN land use scenario resulted in higher in the peak flow as expected, lower baseflow.

Table 5.2 summarizes the results for a completely URBN land use and completely FRST land use class. Subbasin 07362000 has an average flow rate for URBN land use 11.25cms higher than FRST. URBN scenarios resulted in a higher average streamflow by 3.07cms). Similarly, the URBN scenario also resulted in higher peak runoff (e.g., peak flow increased by 106.12 cms higher than FRST run; and low flow were lower for URBN run than the FRST run.

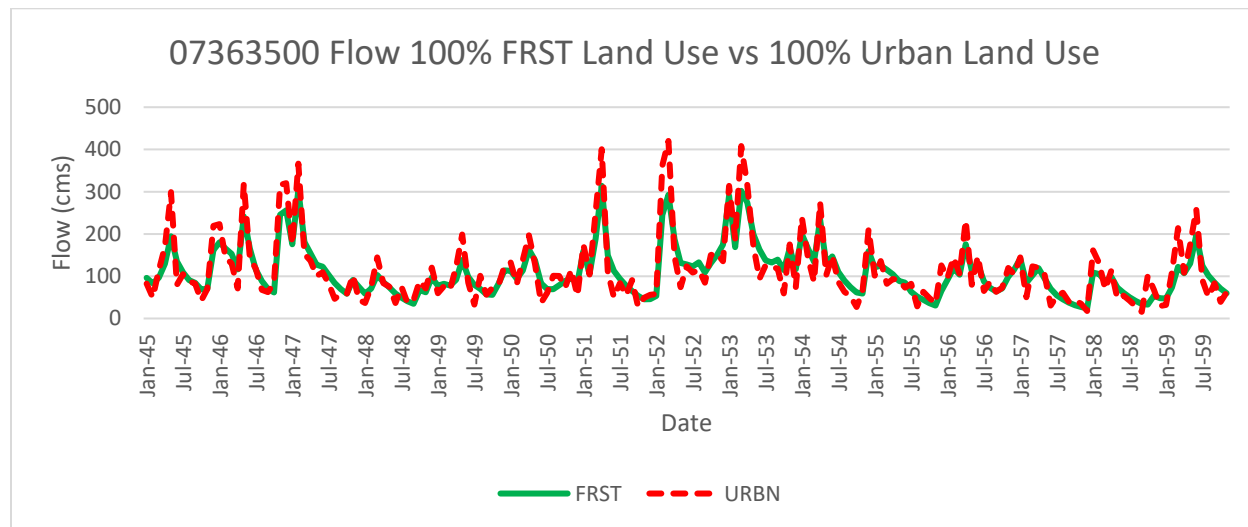


Figure 5.13 Monthly average flow in cubic meters per second for subbasin 07363500 for 100% Forest (FRST) land use and 100% URBN (Urban) land use.

Figures 5.14 summarizes how the monthly streamflow rate are affected when land use is altered from a completely forest land use to a completely urban land use (note that completely urban land use is not realistic and were only used to generate the model response) goes to the extremes as urbanization occurs. As urbanization increases, the surface runoff and subsequently peaks flow increases and consequently the return flow decreases resulting in lower dry weather flow compared to FRST land use simulation. This is also evident in the Table 5.2.

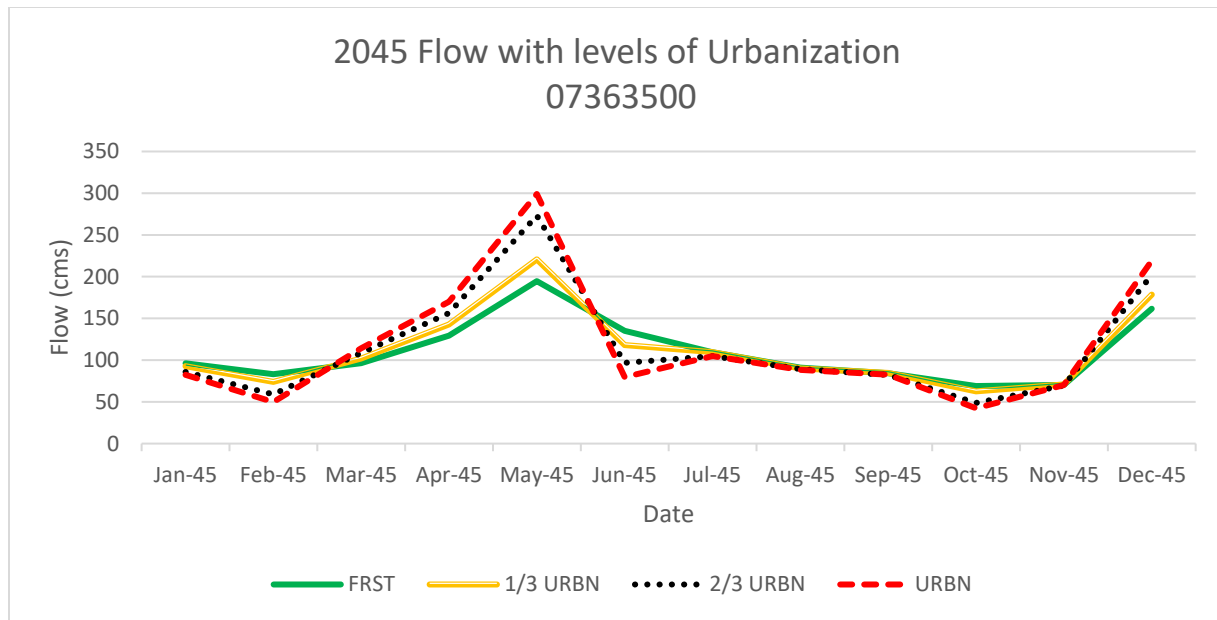


Figure 5.14 Monthly average flow in cubic meters per second in the year 2045 for subbasin 07363500 for varying land uses.

5.2.2 Evapotranspiration

Figures 5.15 shows the simulated actual evapotranspiration (mm/day) with a two extreme land use scenarios i.e., 100% FRST and 100% URBN. For a simulation with 100% URBN, the peaks of the evapotranspiration relatively higher than 100% FRST. However, when the subbasin is 100% FRST, the actual evapotranspiration rate is higher for FRST as compared to URBN. Table 5.2 shows that the average evapotranspiration is 0.05mm/day higher for the FRST land use than the URBN land use for subbasin 07363500. However, the peak streamflow and standard deviation are higher for the URBN.

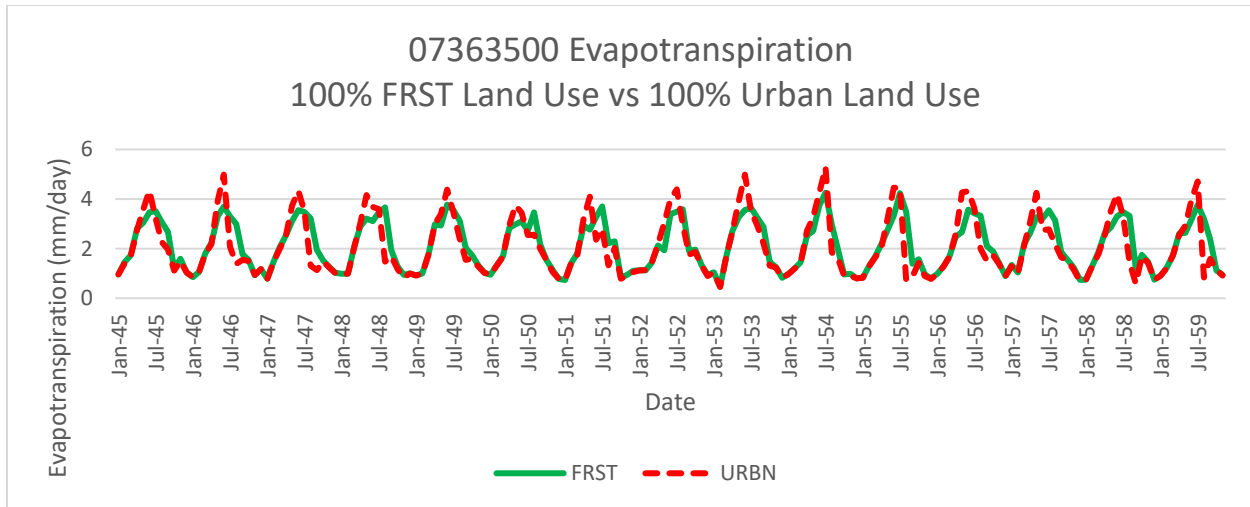


Figure 5.15 Monthly average evapotranspiration in millimeters per day for subbasin 07363500 for 100% Forest (FRST) land use and 100% Urban (URBN) land use.

For comparing the evapotranspiration component, only the 100% FRST and 100% URBN land uses were analyzed (Figure 5.16).

As seen in the figure, the simulation with URBN scenario resulted in a higher peak. The Evapotranspiration quickly increases due to gain of impervious surfaces, and then decreased. However, in the URBN land uses run, the peak value of evapotranspiration occurred at a later time.

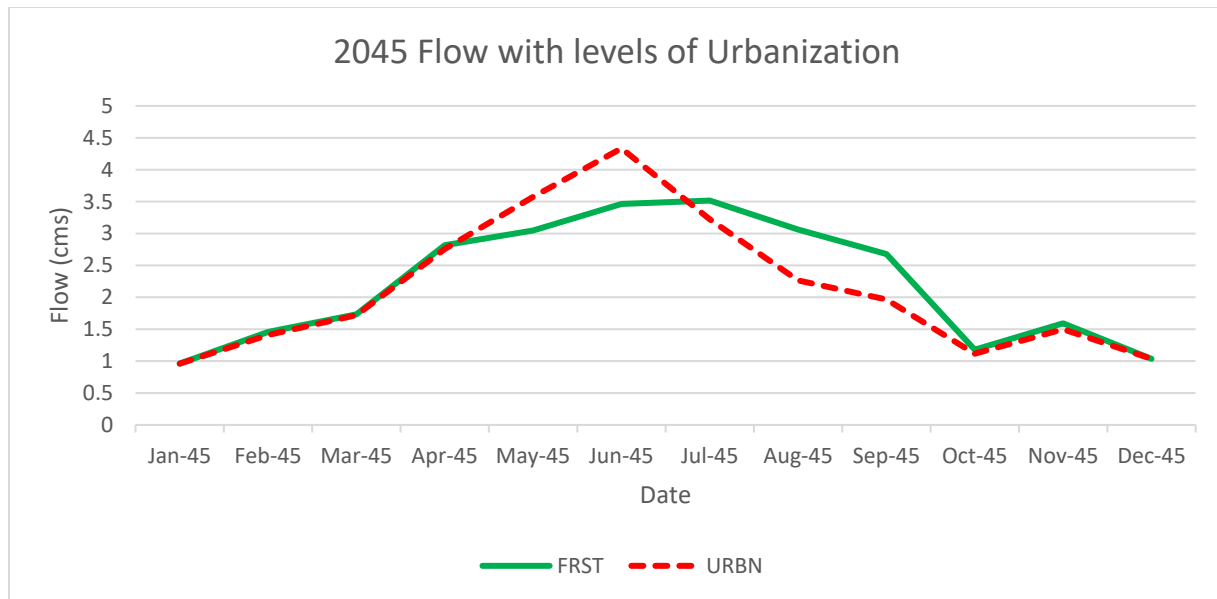


Figure 5.16 Monthly average evapotranspiration in millimeters per day second in the year 2045 for subbasin (USGS ID 07363500) for two land use scenarios (completely Forest (FRST) and Completely urban (URBN)).

5.2.3 Groundwater flow

Figure 5.17 shows the groundwater flow (mm/day) of subbasins 07362000 and 07363500 with a land use of 100% Forest (FRST) and 100% urban (URBN). This graph shows that when the subbasin has 100% FRST land use, the groundwater is higher than when the area is 100% URBN. This is confirmed by the higher average groundwater flow seen in Table 5.2.

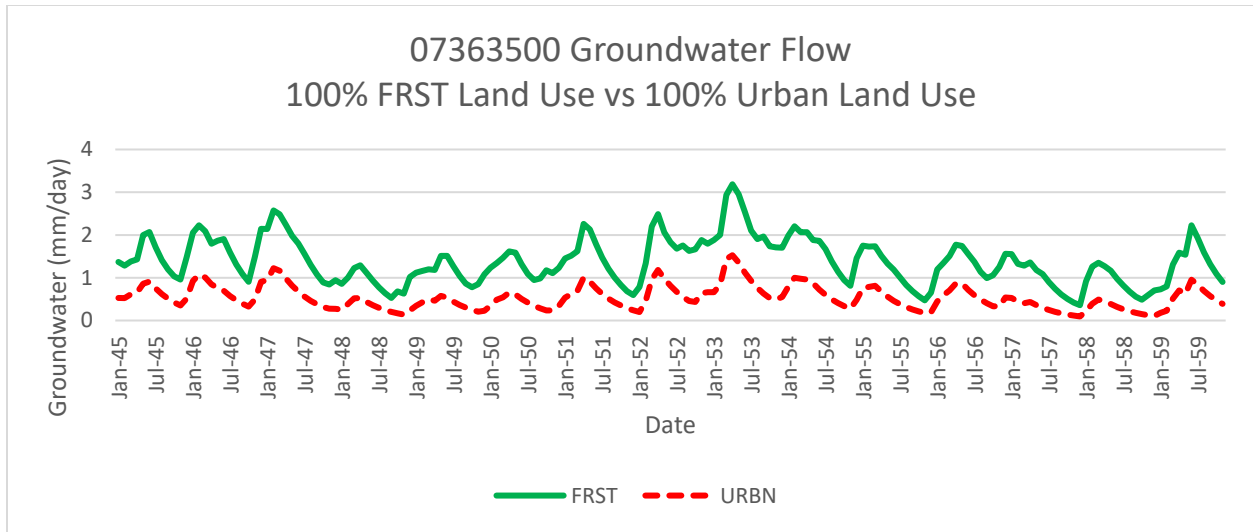


Figure 5.17 Monthly average groundwater flow in millimeters per day for subbasin 07363500 for 100% Forest (FRST) land use and 100% (URBN) Urban land use.

Figures 5.18 shows the groundwater flow for the year 2045 with one complete urbanization and another complete forest scenario. The groundwater flow is lower for higher urbanized land use.

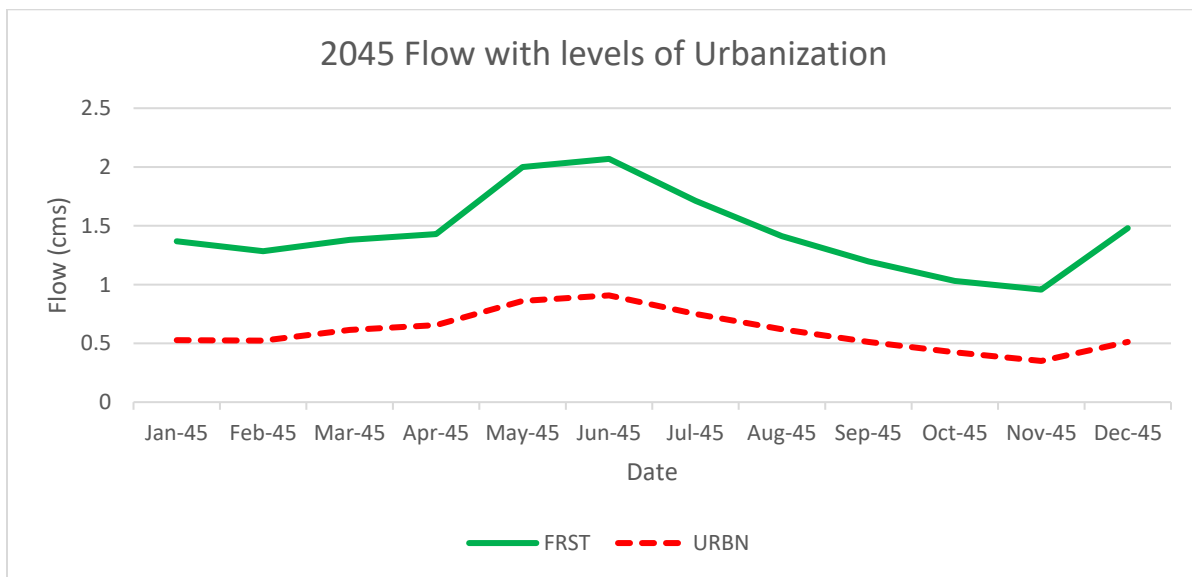


Figure 5.18 Monthly average groundwater flow in millimeters per day second in the year 2045 for subbasin 07363500 for varying land uses.

Chapter 6: Summary and Conclusion

Different component of hydrologic processes (for example streamflow rate, evapotranspiration, and ground water flow) are affected by changes in climate, time period, and land use.

The hydrological simulation between the 2040s and 2080s run with RCP 2.6 and RCP 8.5 show the following. The simulation for 2040s closely followed each other. However, differences in different hydrological component were apparent for the period of 2080s. The study used KNMI climate change atlas to derive temperature maps for this area (Figures 4.3-4.6), both the 2040 and the 2080 period the projected temperature for RCP 2.6 is 1 and 1.5 degrees Celsius warmer for the US. For the same 2040 data, the projected temperature with an RCP 8.5 is 1.5 to 2 degrees Celsius warmer for US. However, for 2080 time period the projected temperature with an RCP 8.5 scenarios is 4 to 5 degrees warmer than historical temperatures.

The USACE's climate hydrology map for temperature (figure 4.7) shows a very similar trend. Additionally, the USACE's climate hydrology map for precipitation (figure 4.8) shows consistently similar precipitation from 2040-2100 with RCP 2.6. Similar values of precipitation changes were observed for RCP 4.5 and RCP 8.5 for the year 2040. Simulation with RCP 4.5 has more variability and the simulation for RCP 8.5 data had larger peaks.

As the projected model for 2040s were not apparently different for different scenarios in order to cause large change in hydrological component. However, apparent changes were observed between the 2040 and the 2080 data for RCP 2.6.

The simulation for the period 2080s with RCP 8.5 was apparently different from 2040s simulation run with RCP 2.6 scenarios. While the evapotranspiration is higher in the RCP 8.5 scenario simulation, the streamflow and ground water are both lower. This indicates that more

water is evaporated consequently reducing streamflow (note that there is no clear signal in an increasing trend in precipitation).

The urbanization experiment show that, an increased urbanization resulted in an increase in streamflow. However, it was also observed that as the urbanization percentage increased, not only did the peak streamflow rates increase, but also an increase in the streamflow variability was observed. Due to an increase in impervious surface, less water is infiltrated into the ground subsequently affecting the return flow or groundwater flow. The urban scenario shows a decrease in the groundwater and as well as a quicker response than the landscape dominated by forest. In both scenarios, the amount of water being transported through evapotranspiration in both a forested and urbanized subbasin are similar in magnitude. However, in the urbanized subbasin, the water is evaporating faster due to the water being evaporated from impervious sources in comparison to forested land use where a great amount of evapotranspiration comes from plants.

Most of the results observed in the experiment were expected and are general. Though the results from the experiment were derived for the specific basin, similar trend may be observed in the nearby subbasin.

The following conclusions found in this research are summarized below:

1. The impact of long term (2080s) projected climate change with extreme scenarios (RCP 8.5) on different components of the hydrological cycle is apparent..
2. Urbanization has an apparent impact on different components of the hydrological cycle e.g., the increase in urbanization rate led to an increase in streamflow rate, increase in peak streamflow and reduction in dry weather flow.
3. With greater rise in temperature, actual evapotranspiration will increase. The magnitude of increase is larger for extreme RCP scenarios and for long horizon projection (2080s).

4. In the selected river basin, ground water flow decreased in in RCP 8.5 and for long horizon projection. Also, the groundwater flow reduced as more forested area is converted into urban land class.

Chapter 7: Recommendations for Future Research

The results of this study show how changing model forcing (e.g., drivers of models such as rainfall, temperature, and the physical system of model such as land use) can affect different component of hydrological cycle, e.g., stream flow, groundwater flow, and evapotranspiration.

This research can be conducted in watersheds further north in the Mississippi River Basin to determine how the projected climate change and land use changes outside of Arkansas will change the hydrological processes and influence the downstream Mississippi River. The research only utilized a single model forcing (temperature and precipitation). The future study can use multiple data sources (publicly available, satellite derived data, reanalysis product) and study how the uncertainty in model input affects and influences the model simulation. Also, the future study can explore using different hydrological components (satellite derived evapotranspiration, groundwater flow measurement from the basin, soil moisture measurement, flow measurement at interior location) for model calibration and validation. Future study can explore the cause of the poor model simulation performance observed in this study.

The land use in areas further north as well as in more populated areas will differ greatly than the land uses used in this study. Exploring how these more realistic land uses scenarios could provide more insight into land use management decision making process. Additionally, the projected climate change in areas further north will differ. Also, the future climate change experiment, which were studied using synthetically generated climate change scenarios in marksim (used in this study covers whole globe and especially developed for agricultural decision making process), could be improved by utilizing statically or dynamically downscaled daily precipitation and temperature projection scenarios, Studying these areas with their local

climate change projections can give a realistic future streamflow projection Mississippi River Basin.

This study can also be expanded by exploring other hydrological processes (crop production, nutrient load, sediment load). The SWAT model can also simulate processes such as the Nitrogen load, Phosphorus load, biomass, chlorophyll transportation, and pesticide movement. Inclusion of wide variety of process can be useful for wide range of decision making process related to management of land and water within the river basin.

The climate change projection experiment is based on the assumption that model parameters are time invariant i.e., the calibration model parameters do not vary in time. This is only true by assumption and may not be realistic to use the model parameters calibrated using historical data to make projection for future where the climate and environment may be very different from the calibration period climate. The study can also be expanded to study the non-stationarity in the calibrated model parameters.

References

- Abbaspour,,K.C. “SWAT-CUP-2012. SWAT Calibration and uncertainty program- A User’s Manual.” Swiss Federal Institute of Aquatic Science and Technology. 2012.
- Afinowicz, J. D., C. L. Munster, and B. P. Wilcox. 2005. Modeling effects of brush management on the rangeland water budget: Edwards Plateau, Texas. *J. American Water Resour. Assoc.* 41(1): 181-193.
- “Arkansas 2020-2029 Forest Action Plan.” Arkansas Department of Agriculture.
<https://www.agriculture.arkansas.gov/wp-content/uploads/2021/01/Arkansas-Forest-Action-Plan.pdf>
- “Arkansas State Water Plan, Lower Ouachita Basin,” Arkansas Soil and Water Conservation Commission. February, 1987.
https://arwaterplan.arkansas.gov/basin%20reports/awp_lower_ouachita_basin.pdf.
- Arnold, J. G., et al., “ Large-area hydrologic modeling and assessment: Part I. Model development,” *J. American Water Resour. Assoc.* 34(1): 73-89. (1998).
- Arnold, J. G. and N. Fohrer. “SWAT2000: Current capabilities and research opportunities in applied watershed modeling,” *Hydrol. Process.* 19(3): 563-572. (2005).
- Arnold, J.G. et al., “Soil & Water Assessment Tool; Input/Output Documentation Version 2012” Texas Water Resources Institute. <https://swat.tamu.edu/media/69296/swat-io-documentation-2012.pdf>.
- Arnold, J. G. et al., “SWAT: Model use, calibration, and validation,” *Transactions of the ASABE* 55, No. 4 (2012).
- Arhonditsis et al., “Castles built on sand or predictive limnology in action? Part B: Designing the next monitoring- modelling- assessment cycle of adaptive management in Lake Earie.” *Ecological Informatics* 53. (2019).

Ashine, Etefa Tilahun and Bedane, Minda Tadesse, “Most Sensitive Parameters of Soil and Water Assessment Tool (SWAT) Hydrologic Model: A Review.” *Advances in Oceanography & Marine Biology*. August (2022).

Betrie, G. D. et al., “Sediment management modelling in the Blue Nile Basin using SWAT model,” *European Geoscience Union* 15, No. 3 (2011).

Budyko, M.I., “The effect of solar radiation variations on the climate of the earth,” *Tellus* 21. (1969).

“Climate Data Online Search.” NOAA. <https://www.ncdc.noaa.gov/cdo-web/search>.

“Climate Hydrology Assessment Tool.” USACE Climate Preparedness and resilience. <https://climate.sec.usace.army.mil/chat/>

Coffey, M. E. et al., “Statistical procedures for evaluating daily and monthly hydrologic model predictions.” *Trans. ASAE* 47(1): 59-68. (2004).

“Cooperative Observer Program.” National Weather Service. <https://www.weather.gov/coop/overview>

Cousino et al., “Modeling the effects of climate change on water, sediment, and nutrient yields from the Maumee River watershed.” *Journal of Hydrology” Regional Studies* Vol 4 Part B. September (2015).

Daughtry et al., “Remote Sensing of Soil Carbon and Greenhouse Gas Dynamics across Agricultural Landscapes,” *Managing Agricultural Greenhouse Gases*, 2012.

“Hydrological Modelling with SWAT.” BTU. November (2020).

Du, B. et al., “Development and application of SWAT to landscapes with tiles and potholes.” *Trans. ASAE* 48(3): 1121-1133. (2005).

“Hypoxia Task Force Action Plan and Goal Framework.” EPA, <https://www.epa.gov/ms-hf/hypoxia-task-force-action-plans-and-goal-framework>.

“KNMI Climate Change Atlas.” Climate Explorer. http://climexp.knmi.nl/plot_atlas_form.py.

Moriasi, et al., “Model evaluation guidelines for systematic quantification of accuracy in watershed simulations,” *Trans. ASABE* 50(3): 885-900. (2007).

“RCP 2.6.” Climate Watch. <https://www.climatewatchdata.org/pathways/scenarios/198>

“Third Gulf of Mexico Hypoxia Task Force Report to Congress Published.” NCCOS. <https://coastalscience.noaa.gov/news/third-gulf-of-mexico-hypoxia-task-force-report-to-congress-published/>.

Du, B. et al., “Development and application of SWAT to landscapes with tiles and potholes.” *Trans. ASAE* 48(3): 1121-1133. (2005).

Gassman, P.W. et al., “The Soil and Water Assessment Tool: historical development, applications, and future research directions,” *American Society of Agricultural and Biological Engineers* Vol. 50. (2007).

“Geospatial Data Gateway.” United States Department of Agriculture. https://datagateway.nrcs.usda.gov/GDGHome_CheckOrder.aspx.

Gobler, Christopher J., “Climate Change and Harmful Algal Blooms: Insights and perspective,” *Harmful Algae* 91, (2020).

“Hydrologic Modeling System, HEC-HMS User’s Manual Version 4.6.” US Army Corps of Engineers Hydrologic Engineering Center. file:///C:/Users/amei/Downloads/HEC-HMS%20User's%20Manual-v41-20230414_103030.pdf.

“Hypoxia Task Force Action Plan and Goal Framework.” EPA, <https://www.epa.gov/ms-hf/hypoxia-task-force-action-plans-and-goal-framework>.

“KNMI Climate Change Atlas.” Climate Explorer. http://climexp.knmi.nl/plot_atlas_form.py.

Moriasi, et al., “Model evaluation guidelines for systematic quantification of accuracy in watershed simulations,” *Trans. ASABE* 50(3): 885-900. (2007).

Kour, Retinder and Patel, Nilanchal, “Climate and hydrological models to assess the impact of climate change on hydrological regime: a review,” *Arabian Journal of Geosciences* 9, 544 (2016).

MarkSim. “MarkSim DSSAT weather file generator.”

<http://gisweb.ciat.cgiar.org/MarkSimGCM/#tabs-1>

Miller, S. N., W. G. Kepner, M. H. Mehaffey, M. Hernandez, R. C. Miller, D. C. Goodrich, K. K. Devonald, D. T. Heggem, and W. P. Miller. 2002. Integrating landscape assessment and hydrologic modeling for land cover change analysis. *J. American Water Res. Assoc.* 38(4): 915-929.

Moody, John A. and Battaglin, William A., “Setting: Chemical character of the Mississippi River,” *U.S. Geological Survey Circular* 1133, (1995).

Muttiah, R. S., and R. A. Wurbs. “Modeling the impacts of climate change on water supply reliabilities,” *Water Intl., Intl. Water Resources Assoc.* 27(3): 407-419. (2002).

Neupane, R.P. and Kuma, S., “Estimating the effects of potential climate and land use changes on hydrological processes of a large agricultural dominated watershed,” *Journal of Hydrology* 529, (2015).

“Ouachita River at Camden, AR – 07362000.” USGS. <https://waterdata.usgs.gov/monitoring-location/07362000/#parameterCode=00065&period=P7D>.

Ougahi et al., “Application of the SWAT model to assess climate and land use/cover change impacts on water balance components of the Kabul River Basin, Afghanistan.” *Journal of Water & Climate Change* 13(11). (2022).

Parajuli, Prem, “Assessing sensitivity pf hydrologic responses to climate change from forested watershed in Mississippi,” *Hydrological Processes* 24, 3785-3797 (2010).

Phung, Quang A. et al., “Climate and land use effects of hydrologic processes in a primarily rain-fed, Agricultural watershed,” *Journal of the American Water Resources Association*, (October 2019).

“Saline River Near Rye, AR- 07363500.” USGS. <https://waterdata.usgs.gov/monitoring-location/07363500/#parameterCode=00065&period=P7D>.

“RCP 2.6.” Climate Watch. <https://www.climatewatchdata.org/pathways/scenarios/198>

“Third Gulf of Mexico Hypoxia Task Force Report to Congress Published.” NCCOS. <https://coastalscience.noaa.gov/news/third-gulf-of-mexico-hypoxia-task-force-report-to-congress-published/>.

Santhi, C. et al., “A modeling approach to evaluate the impacts of water quality management plans implemented in a watershed in Texas,” *Environmental Modelling & Software* 21, No. 8 (2006).

Sellers, W.D. (1969) “A global climate model based on the energy balance of the earth-atmosphere system,” *J Appl Meteorol* 8:392. (1969).

Serpa, D. et al., “Impacts of Climate and Land Use Changes on the Hydrological and Erosion Processes of Two Contrasting Mediterranean Catchments.” *Science of the Total Environment* 538, (2015).

“The Mississippi/ Atchafalaya River Basin (MARB).” United States Environmental Protection Agency. Last modified March 14, 2023. <https://www.epa.gov/ms-hf/mississippiatchafalaya-river-basin-marb>.

White, M.J. et al., “Nutrient delivery from the Mississippi River to the Gulf of Mexico and effects of cropland conservation,” *Journal of Soil and Water Conservation* 69, (January 2014).

Vita

Amelie Lagarde was born in New Orleans, Louisiana. She obtained her Bachelor's degree in environmental engineering from the University of Alabama in 2020. She began her studies at the University of New Orleans in August of 2021 to pursue a Master's degree in Civil and Environmental Engineering with a Coastal Engineering Graduate Certificate. She became a graduate research student for Dr. Satish Bastola in August 2022.